IN THE UNITED STATES PATENT AND TRADEMARK OFFICE

Applicant:	Gjerset et al
Title:	TUMOR SUPPRESSION THROUGH BICISTRONIC CO-EXPRESSION OF P53 AND P14ARF
Appl. No.:	10/717,845
Filing Date:	11/19/2003
Examiner:	Priebe, S.D.
Art Unit:	1633
Conf. No.	9478

DECLARATION OF DR. RUTH GJERSET
UNDER 37 C.F.R. § 1.132

I, Ruth Gjerset, Ph.D., state and declare as follows:

1. I am currently Associate Professor for the Sidney Kimmel Cancer Center, San Diego, CA, the assignee of the above-referenced U.S. Patent Application No. 10/717,845 (hereinafter referred to as "the '845 application"). I am named as a co-inventor on the '845 application. I received a Ph.D. in 1977 from the University of California, San Francisco in Biochemistry and Biophysics and have extensive post-doctoral training in Biochemistry and Molecular Biology at the Pasteur Institute in Paris, and at the University of California, San Francisco and San Diego. I have worked in cancer genetics research for 20 years and have published over 39 scientific articles in peer-reviewed journals and review publications. My curriculum vitae was provided in my earlier declaration of record in this case.

2. I provide herewith evidence to shows that the bicistronic Adp14/p53 vector with the gene encoding p14ARF in the first cistron position and the gene encoding p53 in the second cistron position is an orientation that surprisingly results in enhanced translation of the p53 protein compared to the single gene p53 vector or compared to a combination of p14ARF and

p53 single gene vectors. I also show that this results from a differential effect of p14ARF on CAP-independent translation versus CAP-dependent. This evidence means that the position of the p53 following the IRES in p14/ARF/p53 bicistronic vector is critical to achieve maximal p14ARF and p53 levels in transfected cells. This evidence also explains why, as was shown in my previous declaration, bicistronic Adp14/p53 vector with the gene encoding p14ARF in the first cistron position and the gene encoding p53 in the second cistron position is an orientation that surprisingly results in 40 times the efficacy of the combination of p14ARF and p53 single gene vectors. For the benefit of the Examiner, I attach herewith an article by Hennecke et al. (Nucleic Acid Res. 29:3327-3334 2001), which discusses CAP-dependent and CAP-independent mechanisms of eukaryotic expression.

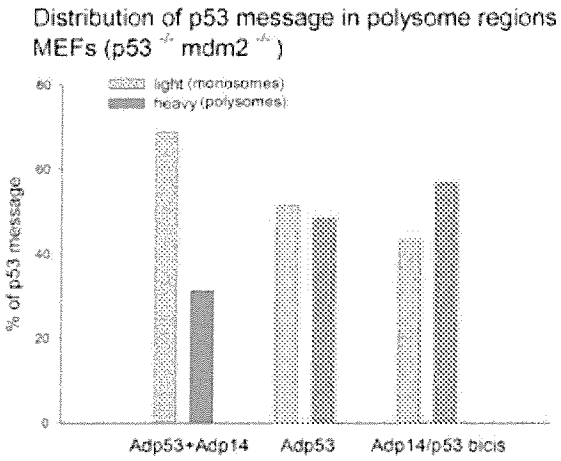

FIGURE 1

3. The level of p53 message was evaluated for various vectors transfected into mouse embryo fibroblasts (MEFs) from p53-null and mdm2-null mice. Cells were treated with Adp53 single gene vector, Adp14/p53 bicistronic vector, or combination of p14ARF and p53 single gene vectors (Adp53 + Adp14). Polysomes were prepared and fractionated and two pools were analyzed for p53 message (light = monosome region; heavy = polysome region). The results are shown in Figure 1. In Adp53-treated cells, where p53 message is translated in a CAP-dependent manner, p53 message is evenly distributed between light and heavy polysome

fractions. In (Adp14 + Adp53)-treated cells, where p53 is also translated in a CAP-dependent manner, p53 message is found preferentially in the light polysome region, i.e., poorly translated. This is consistent with published studies showing that p14ARF suppresses CAP-dependent cellular translation (see, e.g., Rizos, H., et al. (2006) J. Biol. Chem. 281:38080-38080) (attached as Exhibit B). Finally, in Adp14/p53 bicistronic vector-treated cells, where p53 translation occurs in a CAP-independent manner from the IRES, p53 message distribution is shifted slightly toward the heavy polysome region, and the strong translational suppression by p14ARF that was observed with the combination of single gene vectors is now absent.

4. I conclude from the results that p53 is efficiently translated when it is placed downstream of an IRES in a bicistronic construct, even in the presence of p14ARF. Thus, the suppressive effect of p14ARF on translation (see, e.g., Rizos, H., et al. (2006) J. Biol. Chem. 281:38080-38080), which arises from its natural endogenous expression or as a result of vector expression is reduced or eliminated for p53 placed downstream of an IRES. Because p14ARF plays competing roles with regard to p53 accumulation, the positive effect of p14ARF on p53 accumulation (via protein stabilization) will be attenuated by its negative effect on translation.

5. The beneficial effects of enhanced p53 expression when expressed from the IRES in the P14ARF/p53 bicistronic construct is unexpected and explains why, as was shown in my previous declaration, bicistronic Adp14/p53 vector with the gene encoding p14ARF in the first cistron position and the gene encoding p53 in the second cistron position is an orientation that surprisingly results in 40 times the efficacy of the combination of p14ARF and p53 single gene vectors.

6. I have not directly compared p53 translation in a bicistronic P14ARF-IRES-p53 versus p53-IRES- P14ARF. However, I believe such experiment is not needed because CAP-dependent expression of p53 from the forward position in the bicistronic vector should be impacted negatively by P14ARF expressed from CAP-independent position following the IRES in the bicistronic vector.

7. I am familiar with US Patent No. 6,060,273 by Dirks and I conclude that it teaches away from my invention because Dirks teaches the well known fact that when using bicistronic vectors with an IRES element, expression for the second and subsequent cistrons is

impacted negatively by P14ARF expressed from CAP-independent position following the IRES in the bicistronic vector.

7. I am familiar with US Patent No. 6,060,273 by Dirks and I conclude that it teaches away from my invention because Dirks teaches the well known fact that when using bicistronic vectors with an IRES element, expression for the second and subsequent cistrons is always deficient compared to expression from the first "CAP-dependent" cistron. Dirks, column 2-3. Although it is appreciated that transfection with both p53 and p14ARF is better than use of each gene separately, the most important of the two genes is p53. Thus, if one were motivated to make as bicistronic vector with p14ARF and p53, one would from the teaching of Dirks choose to put p53 in the CAP-dependent position directly following the promoter and p14ARF in the 2nd cistron following the IRES. This would be done on the belief that one would get greater p53 expression than in the reverse and achieve better overall therapy than when p53 is placed in the second cistron position.

8. I further declare that all statements made herein of my own knowledge are true and that all statements made on information and belief are believed to be true; and further that these statements are made with the knowledge that willful false statements so made are punishable by fine or imprisonment or both under § 1001 of Capital Title 18 of the United States Code, and that such willful false statements may jeopardize the validity of the application or any patent issuing thereon.

March 2, 2009
Date

Ruth Gjerset, Ph.D.

Nucleic Acids Research, 2001, Vol. 29, No. 16 3327–3334

Composition and arrangement of genes define the strength of IRES-driven translation in bicistronic mRNAs

Meike Hennecke, Marcin Kwissa[1], Karin Metzger[1], André Oumard, Andrea Kröger, Reinhold Schirmbeck[1], Jörg Reimann[1] and Hansjörg Hauser*

Department of Gene Regulation and Differentiation, GBF–German Research Center for Biotechnology, Mascheroder Weg 1, D-38124 Braunschweig, Germany and [1]Institut für Medizinische Mikrobiologie, Universität Ulm, Albert-Einstein-Allee 11, D-89069 Ulm, Germany

Received May 18, 2001; Revised and Accepted July 2, 2001

ABSTRACT

In addition to the cap-dependent mechanism, eukaryotic initiation of translation can occur by a cap-independent mechanism which directs ribosomes to defined start codons enabled by internal ribosome entry site (IRES) elements. IRES elements from poliovirus and encephalomyocarditis virus are often used to construct bi- or oligocistronic expression vectors to co-express various genes from one mRNA. We found that while cap-dependent translation initiation from bicistronic mRNAs remains comparable to monocistronic expression, internal initiation mediated by these viral IRESs is often very inefficient. Expression of bicistronic expression vectors containing the hepatitis B virus core antigen (HBcAg) together with various cytokines in the second cistron of bicistronic mRNAs gave rise to very low levels of the tested cytokines. On the other hand, the HBcAg was well expressed when positioned in the second cistron. This suggests that the arrangement of cistrons in a bicistronic setting is crucial for IRES-dependent translation of the second cistron. A systematic examination of expression of reporter cistrons from bicistronic mRNAs with respect to position was carried out. Using the dual luciferase assay system we show that the composition of reading frames on a bicistronic mRNA and the order in which they are arranged define the strength of IRES-dependent translation. Although the cellular environment and the nature of the IRES element influence translation strength the dominant determinant is the nature and the arrangement of cistrons on the mRNA.

INTRODUCTION

Internal initiation of translation mediated by internal ribosome entry site (IRES) elements (1) in artificial expression constructs has enabled the development of expression vectors in which two or more unrelated reading frames are expressed from a single transcription unit (2–5). The major advantage of this technique, which occurs naturally in prokaryotes but has not been detected in higher eukaryotes, lies in strict co-expression of transgenes *in vitro*, in cell culture and transgenic animals and plants (6–10). Furthermore, it avoids the side-effects of using multiple promoters in vectors with limited size retroviral vectors (11–14).

IRES elements have been isolated from picornaviruses (15,16), other animal viruses (e.g. hepatitis C virus, hepatitis A virus and retroviruses) and mammalian and *Drosophila* RNAs (17–26). They differ in their primary sequence. Some IRES elements show similarities in their secondary structures (27,28). In several picornaviruses the internal entry process seems to require the cellular polypyrimidine tract-binding protein (PTB) (29), but PTB binding does not necessarily correlate with its activity (30). It seems that the activity of IRES elements is controlled by different cellular factors (31,32). Since the known IRES elements show differential activity and their activity depends on cell type (33), the composition of cellular factors binding to IRES elements is responsible for translation efficiency.

The strength of translation initiated from different IRES elements differs significantly (7,33,34). The IRES elements from poliovirus and encephalomyocarditis virus (EMCV) are most commonly used for construction of bicistronic expression constructs and vectors (3,35). Making use of IRES elements, tri- and polycistronic expression cassettes can be constructed. Some examples of tricistronic expression have been published (see for example 36–38).

It is generally believed that the strength of internal translational initiation is defined by the nature of the IRES element and the cellular context. However, construction of many bi- and oligocistronic expression constructs has shown us that other parameters resulting from construction of the vectors strongly influence IRES efficiency. This would indicate that protein expression from artificial oligocistronic expression units cannot be predicted. Here we describe some of these observations. In experiments with more defined conditions using the dual luciferase system we show that the constellation of two reading frames in a bicistronic expression setting can

*To whom correspondence should be addressed. Tel: +49 531 6181 250; Fax: +49 531 6181 262; Email: hha@gbf.de

alter IRES-dependent translation from different IRES elements by orders of magnitude. This indicates that the nature of the reading frames assembled on one transcription unit dictates the strength of IRES-dependent translation. Further experiments suggest that the nature of the first cistron defines the strength of downstream IRES-dependent translation.

MATERIALS AND METHODS

Plasmid constructs

Constructions were carried out by standard molecular cloning techniques (39). All of the bicistronic plasmids of the pCI series are based on the pCI backbone (Promega). All bicistronic plasmids of the pBS or pBC series are derivatives of pSBC-1 and -2 (3).

Two new vectors based on pSBC were constructed. pMS, a monocistronic expression plasmid contains the SV40 promoter and a downstream multiple cloning site (MCS), followed by a unique *Not*I site. The second monocistronic plasmid, pMSP, is identical to pMS except that the poliovirus-derived IRES sequence is inserted between the promoter and MCS. The fragment spanning from the IRES to the MCS is flanked by two *Eag*I sites. In the monocistronic plasmid pMC the SV40 promoter in pMS was exchanged for the human cytomegalovirus (CMV) immediate-early enhancer/promoter region derived from pCI. After introducing the gene(s) of interest (e.g. Fluc, Fluz, Rluc or cat) into the MCS of the monocistronic vectors, bicistronic expression plasmids were created by inserting the IRES plus the gene of interest as *Eag*I fragments from pMSP into *Not*I-restricted monocistronic plasmids derived from pMS or pMC. This cloning step results in a single *Not*I site 3′ to the second cistron in the bicistronic constructs. This allows generation of tri- and oligocistronic vectors by adding further *Eag*I fragments from monocistronic pMSP plasmids (35).

Monocistronic expression vectors of the pMSP type carrying the EMCV-derived IRES sequence in combination with the gene of interest were constructed using overlap extension PCR in order to fuse the start codon in the correct position.

All hepatitis B virus core antigen (HBcAg) and cytokine expressing vectors are based on the pCI plasmid backbone. The poliovirus IRES sequence containing the MCS site from pVBC-3 (40) was cloned into pCI using *Eco*RI and *Not*I, resulting in plasmid pCI P, which contains *Eco*RI and *Sal*I sites upstream and a *Not*I site downstream of the IRES sequence.

The HBcAg sequence (40,41) was blunt-end cloned into pCI P using Klenow-treated *Sal*I to create the monocistronic pCI HBc vector containing the poliovirus IRES downstream of the HBcAg. The cytokine genes IFNγ and GM-CSF (42,43) were introduced downstream of the IRES using the *Not*I site of pCI HBc, creating bicistronic pCI Cyt P HBc vectors encoding HBcAg and either cytokine.

To construct monocistronic plasmids expressing IFNγ or GM-CSF, the gene of interest was introduced into pCI P using *Eco*RI and *Sal*I. The HBcAg encoding sequence was cloned downstream of the IRES into the monocistronic *Not*I site of cytokine-expressing vectors, resulting in bicistronic pCI Cyt P HBc vectors.

The IL-12 subunit p35 and p40 genes were cloned into vector pCI P upstream of the IRES sequence to create monocistronic constructs pCI p35 and pCI p40, respectively. Bicistronic vectors pCI-p35-P p40 and pCI p40 P p35 were constructed by inserting either the p40 or p35 gene downstream of the IRES into pCI p35 and pCI p40, respectively.

Series of bicistronic constructs with reporter genes encoding firefly luciferase (Fluc), a synthetic variant of firefly luciferase (Fluz) (Promega), *Renilla* luciferase (Rluc) or chloramphenicol-acetyl transferase (cat) were created. They contain either the poliovirus IRES element (pBSFlucPRluc, pBSRlucPFluc, pBSFluzPRluc, pBCFlucPRluc, pBCRlucPFluc, pBScatPFluc, pBSFlucPcat, pBSFluzPcat, pBScatPRluc and pBSRlucPcat), the EMCV IRES element (pBSFlucERluc, pBSRlucEFluc, pBCFlucERluc and pBCRlucEFluc) or the human NRF IRES (pBSRlucNFluc). The coding sequences of these reporters were derived from de Wet *et al.* (44) for Fluc, from Promega for Rluc and Fluz and from Gorman *et al.* (45) for cat. All PCR created parts of the expression plasmids were verified by DNA sequencing.

Cell culture and transient transfections

Mouse C243 (46), mouse LMTK (ATCC no. CCL 1.3), hamster BHK-21 (ATCC no. CCL-10) and chicken LMH cells (a generous gift of Dr H.-J. Schlicht, Ulm, Germany) were maintained in Dulbecco's modified Eagle's medium (DMEM) with 10% fetal calf serum (FCS), antibiotics and 2 mM glutamine. Murine C2C12 cells (ATCC no. CRL-9096) were cultured in RPMI 1640 (Gibco BRL) supplemented with 5% FCS, antibiotics and glutamine. DNA was transiently transfected using the calcium phosphate co-precipitation method. For reporter gene expression cells from the exponential growth phase were seeded (7.5×10^4 cells) into six-well plates the day before transfection. The medium was changed 4 h prior to transfection and renewed 18 h post-transfection. For transient transfection 1 μg reporter plasmid together with 4 μg high molecular weight DNA from LMTK$^-$ cells per well were used. For transient transfection of the DNA immunisation vectors LMH, BHK-21 and C2C12 cells (2×10^6) were treated with 10 μg plasmid DNA (encoding murine IFNγ, murine GM-CSF and the murine IL-12 p35 and p40 subunits). Transfection efficiency was standardised by co-transfection with one of the monocistronic plasmids expressing either Fluc, Rluc or cat. Two days post-transfection cells or supernatant were harvested and analysed.

All transfections were carried out between three and six times. Although the absolute amounts of expression varied, the standard deviations of the ratios cistron 2/1 were <20%. All data shown derive from representative experiments.

Analysis of gene products

The supernatants were analysed for release of cytokines by conventional double sandwich ELISA as described (42,43). For detection of HBcAg the cells were lysed in PBS containing 1% Triton X-100. Immunoprecipitation was performed using a rabbit anti-C antiserum (αHC1) and protein A–Sepharose. Immune complexes were processed for SDS–PAGE and transferred onto nitrocellulose. Detection of HBcAg was performed using αHX1 and alkaline phosphatase-conjugated anti-rabbit IgG and subsequent staining with BCIP and NBT.

Luciferase activity of firefly and *Renilla* luciferase was measured with the Dual Luciferase System Assay (Promega) according to the manufacturer's instructions. cat analysis was

performed by cat-ELISA (Boehringer Mannheim) as described in the manufacturer's instructions. Mean values from double or triple determinations were taken. Extracts from transfected cells were prepared by passive lysis. The amount of specific first cistron reporter protein expression was normalised to the protein content, which was measured with BCA protein assay reagent (Pierce). Experiments were only considered if transfection efficiency between the different experiments was comparable. Relative expression of two different genes in a bicistronic construct was determined by dividing the value for gene activity of the gene in the second cistron by the value obtained for the gene in the first cistron.

RESULTS

Translation of cytokines in the second cistron is very inefficient

Figure 1A shows the transcription units of expression plasmids encoding the HBcAg and diverse cytokines in monocistronic and bicistronic configurations. Expression of all genes, HBcAg as well as the cytokines positioned in the first cistron and thereby translated in a cap-dependent manner, was clearly detectable. Importantly, no significant differences could be found between mono- and bicistronic configurations (Fig. 1B and C and data not shown). This indicates that comparable steady-state amounts of mRNA from mono- and bicistronic expression plasmids were produced. HBcAg was also well expressed when positioned in the second cistron of the bicistronic expression plasmids (Fig. 1C). The protein amount was ~3- to 10-fold lower when compared to monocistronic expression or if expressed as the first cistron in a bicistronic set-up. This reduction was expected, since earlier data showed that poliovirus IRES-dependent translation was less efficient than cap-dependent translation (47).

In contrast, expression of the cytokines IFNγ and GM-CSF from second cistrons was very low (Fig. 1B). Compared to expression from the first cistron this amounts to a >100-fold difference. The strength of HBcAg expression from these bicistronic mRNAs (Fig. 1C) indicates inefficient IRES-dependent translation of the cytokines tested.

Another example of unexpected low translation from a second cistron was seen when the two peptide chains (p40 and p35) of IL-12 were expressed in a bicistronic manner. p40 was well expressed from monocistronic mRNA or as the first cistron of a bicistronic mRNA. However, it could hardly be detected when it was positioned in the second cistron (Fig. 2).

The above-described key observation, namely inefficiency of IRES-dependent translation of certain cytokines, was found in cell lines from different species.

These observations led us to conclude that IRES-dependent translation is not predictable and obviously depends on the composition of the mRNA. Which RNA elements and other factors, like expression strength, contribute to this phenomenon and if they are of a general nature cannot be deduced from these results. We thus tried to verify these findings with other genes and find principles which allow the prediction of IRES-dependent translation efficiency.

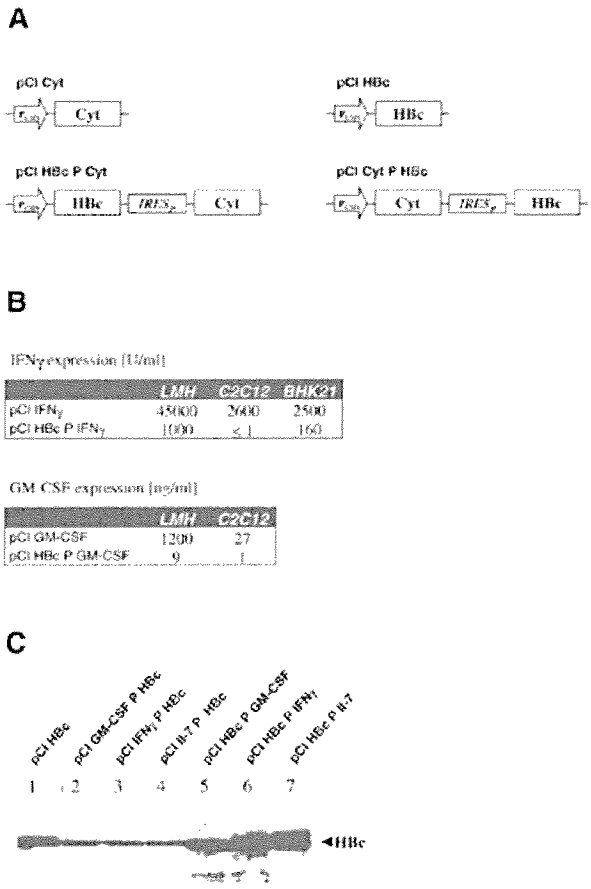

Figure 1. Expression of cytokines and HBcAg (HBc) from mono- and bicistronic mRNAs. (**A**) Schematic diagram of mono- and bicistronic vector constructs (pCI based) used to measure protein expression after transient transfection into different cell lines. P_{CMV} in the open arrow marks the CMV promoter. Cyt indicates the cytokine gene for either IFNγ, GM-CSF or Il-7. $IRES_p$ represents the poliovirus-derived IRES element. (**B**) Determination of IFNγ and GM-CSF in the supernatant of the indicated cells by ELISA. The indicated plasmids were transfected into the cell lines LMH, C2C12 and BHK21 and cytokine concentrations were determined after a transient expression period of 48 h. (**C**) Detection of HBcAg (HBc) in the lysates of LMH cells by western blot analysis. HBcAg was expressed either monocistronically (lane 1), as a first (lanes 5–7) or as a second (lanes 2–4) cistron.

Position-specific expression of two luciferase genes

Reporter systems for which translation was found to be unpredictable from IRES-containing mRNAs are the luciferases from firefly (Fluc) and *Renilla* (Rluc). In our study we have employed both luciferases as reporters for determination of translational efficiency of two reading frames from one mRNA. The composition of different protein coding and non-coding elements in a new context should not only influence transcription, but also mRNA processing, transport, stability, destination and translation (48,49). However, our results showed no significant influence on transcription (data not shown). mRNA stability seems to be dictated by sequence elements which are responsible for rapid degradation. In experiments with the luciferase genes and IRES elements we could detect little influence on the steady-state level (3-fold

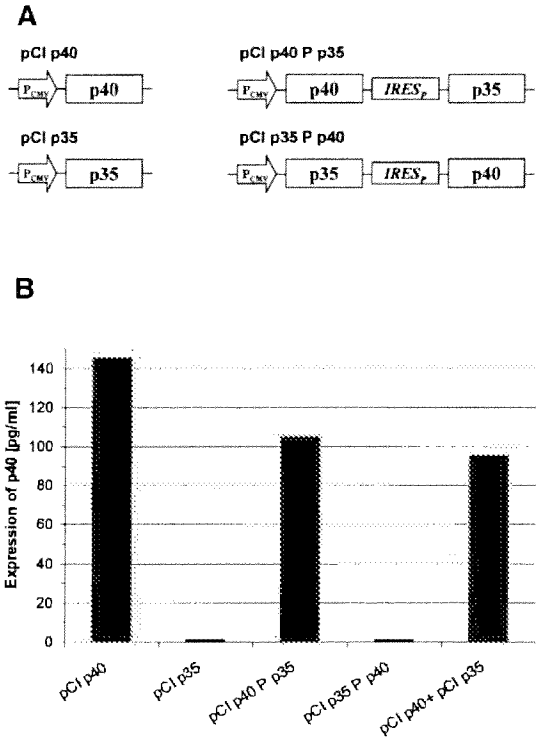

Figure 2. Expression of IL-12 subunit p40 from mono- and bicistronic expression plasmids. (**A**) Schematic presentation of mono- and bicistronic vector constructs used to express the two subunits p35 and p40 of IL-12 in the first or second cistron. The genes encoding p35 and p40 were separated by the poliovirus-derived IRES element ($IRES_P$) and were expressed under control of the CMV promoter (P_{CMV}). (**B**) Detection of the p40 subunit of IL-12 by ELISA. Plasmids as described in (A) were transfected into LMH cells and the gene product of the p40 subunit was determined in the supernatant after a transient expression period of 48 h. One representative experiment from a series of independent experiments with identical results is shown.

maximum) of the mRNAs produced by the constructs (data not shown). Our experiments further confirmed that translation of the first (cap-dependent) cistron paralleled the steady-state level of the respective mRNA but was not significantly influenced by the protein coding sequence on the mRNA. For this reason translation of the cap-dependent reading frame could be used as an internal standard for determination of the strength of IRES-dependent translation of the downstream reading frame(s). The ratio between the luciferase activities from the second and the first cistron defines the strength of IRES-dependent translation. This system, with its high accuracy and low error rate of activity determination, significantly increased the reproducibility of the results from transfection assays.

Figure 3 shows expression of the luciferases from bicistronic mRNAs with various compositions of the same sequence elements in C243 cells. The luciferase values for the first cistrons were very similar irrespective of the gene (Fluc or Rluc) and the existence of a downstream IRES-directed second cistron. This is compatible with the assumption that the stabilities of the newly assembled mRNAs are comparable and that cap-dependent translation is not influenced by the downstream elements. This allowed us to use the quotient ratio of cistron 2/1 expression. Expression of the second cistron, however, was dependent on the arrangement of the luciferases on the mRNA. While IRES-dependent translation of Fluc was very strong, that of Rluc appeared ~30-fold less efficient (Fig. 3B). Thus, expression of the two luciferases reflects the unexpected observations of bicistronic expression of HBcAg and cytokines.

We examined whether this phenomenon could be due to the abundance and composition of cellular factors which influence IRES-mediated translation. This was done by expression of the mRNAs from different promoters and in different cellular backgrounds (Fig. 3C and D, respectively). Indeed, the abundance of steady-state mRNA as judged from expression of the first cistron luciferases differed >10-fold (data not shown). However, the ratio cistron 2/1 was nearly identical. This indicates that specific cellular conditions are not responsible for the differences in IRES-dependent translation. In contrast, it seemed as though the phenomenon is of a general nature.

Influence of the specificity of the IRES element

All bicistronic constructs described above are based on the poliovirus-derived IRES element. We asked whether the nature of the IRES element would influence the efficiency of second cistron translation. Two IRES elements of different origins, types and strengths were used to replace the poliovirus IRES element in the bicistronic expression plasmids. The EMCV-derived IRES element is known to be of similar strength compared to the poliovirus element, although it is classified as a type II IRES (33). The cellular IRES element from the human NRF gene is a type I IRES, but shows superior activity compared to the poliovirus IRES (34). Figure 3E shows the relative expression values from the relevant constructs. Again, IRES-mediated translation of Fluc was strong or very strong in the case of the NRF IRES. However, the inverse orientation of the luciferase cistrons (Fluc-IRES-Rluc) did not allow strong IRES-mediated translation of Rluc. Rluc expression from the second cistron was significantly lower than Fluc expression from the first cistron. The relative efficiency differed amongst the IRES elements. In this conformation IRES-dependent translation is extremely low. Thus, translation from the EMCV IRES showed the best performance. Nevertheless, the phenomenon of mRNA composition-dependent IRES activity was seen with all three IRES elements, indicative of a general mechanism.

Influences of position and sequence of reading frames

Based on the assumption that one of the luciferase cistrons in the bicistronic construct (Fluc-Rluc configuration) exerts a position-dependent negative effect on IRES-mediated translation, bicistronic expression plasmids in which the reporter gene cat replaced either of the luciferases were constructed (Fig. 4A). Constructs composed of cat and Rluc showed efficient IRES-mediated translation in both combinations, indicating that Rluc does not inhibit its own translation when positioned as a second cistron (Fig. 4B). The results further show that cat has no negative effect on IRES-mediated translation in either position. Constructs harboring cat and Fluc exerted strong translation of the downstream Fluc but very low expression of cat as the second cistron (Fig. 4B). These data suggest that the positioning of Fluc in the first cistron position exerts a negative effect on IRES-driven cistrons (cat and Rluc).

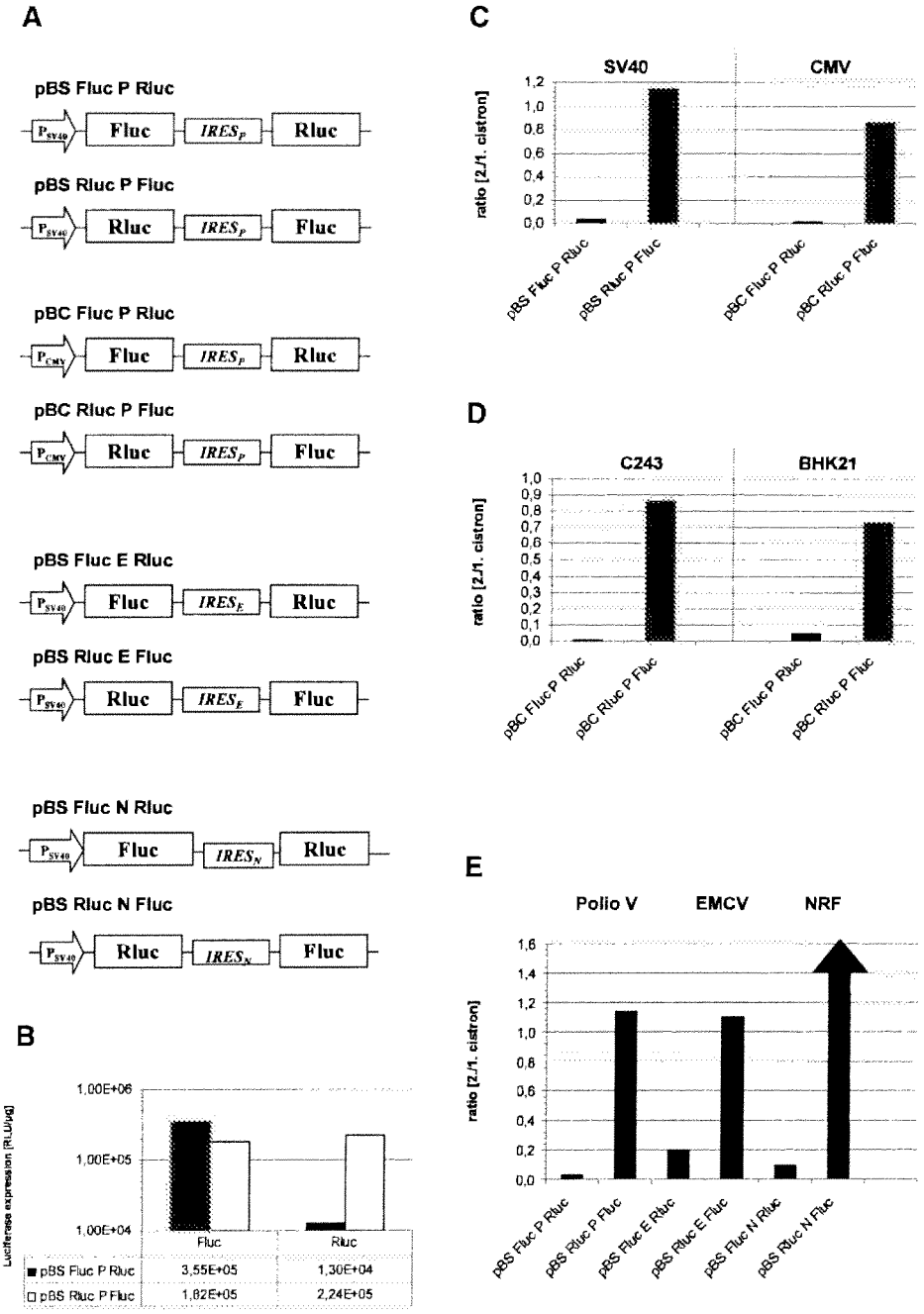

Figure 3. Determination of different parameters affecting expression level of reporter genes in bicistronic constructs. (**A**) Schematic diagram of bicistronic vector constructs used to measure protein expression of firefly and *Renilla* luciferase after transient transfection of C243 cells. P_{SV40} and P_{CMV} in the open arrow mark the SV40 and CMV promoters, respectively. The genes encoding firefly luciferase (Fluc) and *Renilla* luciferase (Rluc) are separated by IRES elements from poliovirus ($IRES_P$), EMCV ($IRES_E$) or huNRF ($IRES_N$). The pSBC vector backbone was used. (**B**) The plasmids pBSFlucPRluc and pBSRlucPFluc were transiently transfected into C243 cells. After 48 h the activities of firefly and *Renilla* luciferase were determined as described in Materials and Methods. One representative from at least six independent experiments with comparable results is shown. (**C**) The same bicistronic transcription units as in (B), driven by either the SV40 promoter (pBS) or the CMV promoter (pBC), were transfected into C243 cells. Activities from Fluc and Rluc were determined as described in (B) and the ratio (cistron 2/1) was determined by dividing the luciferase activities from the second cistron by those derived from the first cistron. The absolute luciferase values for the pBS plasmids are indicated in (B); the values for the first cistron from pBC plasmids were 5×10^6 U/µg for Fluc and 4.5×10^6 U/µg for Rluc. (**D**) The indicated plasmids were transfected into C243 and BHK 21 cells. The samples were assayed and calculated as described in (C). First cistron derived values were 6×10^5 U/µg for Fluc, 7.3×10^5 U/µg for Rluc in C243 cells and 8×10^5 U/µg for Fluc, 9.4×10^5 U/µg for Rluc in BHK21 cells. (**E**) Three sets of bicistronic plasmids containing IRES elements derived from poliovirus, EMCV or human NRF were assayed in C234 cells. The results were plotted as in (C) and (D). Due to the high strength of the NRF IRES element in the Rluc-IRES-Fluc arrangement the calculated ratio of 30 is not depicted to scale. The absolute luciferase values for all first cistron values were between 5.4×10^5 and 7×10^5 U/µg for Fluc and between 3×10^5 and 6.8×10^5 U/µg for Rluc.

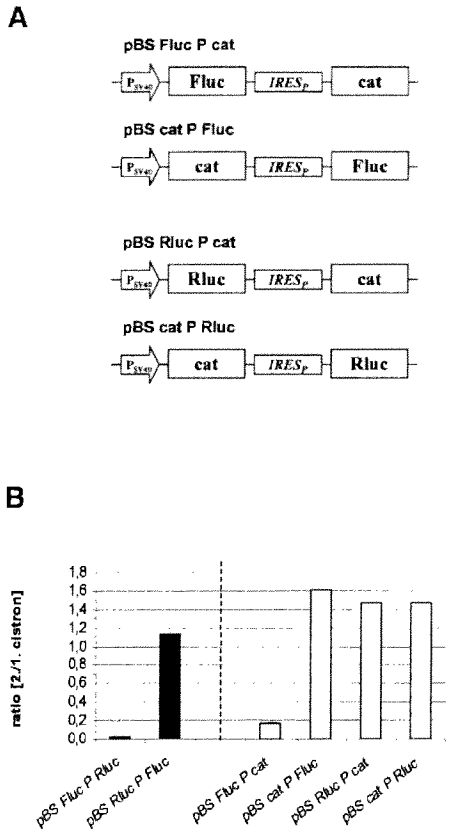

Figure 4. Effect of arrangement of luciferase reporter genes on cap-dependent and IRES-dependent translation. (**A**) Schematic representation of expression constructs used to measure reporter gene expression after transient transfection of C243 cells. (**B**) Expression of firefly luciferase, *Renilla* luciferase and cat from the indicated plasmids were determined. The data in the left half were determined as described in Figure 3C–E. cat values from comparable monocistronic constructs were converted to luciferase analogous values in order to obtain comparable relative expression values. The absolute values for the first cistrons (luciferases) were 3.8×10^5 U/µg for pBS Fluc PRLuc, 2.4×10^5 U/µg for pBS RLuc PFluc, 4.5×10^5 U/µg for pBS Fluc Pcat and 3.6×10^5 U/µg for pBS LucPcat.

In order to determine whether the translation product of Fluc or the translation process as such was responsible for this effect, different experiments were carried out (not shown). First, monocistronic Fluc was co-expressed with pBScatPRluc. The results show no hindrance of Rluc expression, proving that the presence of cellular Fluc RNA or protein does not inhibit IRES-mediated translation of Rluc. Secondly, the poliovirus-derived protease 2A was expressed together with different bicistronic constructs (pBScatPRluc and pBSFlucPRluc). Protease 2A inhibited cap-dependent translation ~3-fold. However, the level of IRES-mediated translation was not significantly altered in these experiments. The ratio cistron 2/1 from pBSFlucPRluc and pBSFlucPcat was increased ~3-fold in the presence of the protease. These data again give no indication of an influence of the cap-dependent Fluc translation process on downstream IRES-mediated translation.

The presented data point towards an influence of sequence or structure of Fluc when positioned upstream of the IRES. Thus, sequence alterations in Fluc in pBSFlucPRluc should lead to a different efficiency of IRES-mediated translation. We used a variant Fluc cDNA, Fluz, in which 76.1% of the coding nucleotide sequence is altered. Fluz replaced Fluc as the first cistron in two bicistronic constructs (Fig. 5). Fluz protein translation showed little alteration in comparison to Fluc and did not change the yield of firefly luciferase activity in C243 cells (data not shown). However, IRES-mediated translation of both Rluc and cat was more strongly reduced (Fig. 5). This indicates that the nucleotide exchanges introduced led to an even stronger negative effect on downstream IRES-mediated translation.

DISCUSSION

Bicistronic expression is frequently used in transgene expression in mammalian cell culture or in transgenic animals where co-expression of heterologous genes is required (35,50). One of the classical applications is the establishment of stable cell lines producing recombinant proteins by co-expression of a selectable marker together with the protein of interest (51). It is further used to achieve overexpression of recombinant proteins in baby hamster kidney (BHK) and Chinese hamster ovary (CHO) cells. Other applications include co-expression of genes which are needed for specific applications, like immunisation to co-express an antigen and a co-stimulatory protein. Although bi- or oligocistronic expression has not yet been convincingly demonstrated as a naturally occurring process in mammalian cells, it is a powerful tool. It is further important to note that many examples of successful bicistronic gene expression have demonstrated IRES-dependent translation of artificial mRNAs. This applies not only to mammalian genes but also to reporter genes from different species. However, failures of bicistronic applications have been observed, although these were often not published. Our motivation was an inability to sufficiently co-express HBcAg antigen and cytokines in DNA immunisation experiments.

With the data shown in this work we demonstrate that synthetic mRNA assembly can exert strong negative effects on IRES-mediated translation. Our data indicate that certain coding sequences can exert a negative effect on IRES-mediated translation, e.g. those encoding the HBcAg and two firefly luciferases. Cap-dependent translation was little influenced by the assembly of the cistrons and IRES elements on the mRNA. This does not mean that cap-dependent translation is completely independent of the mRNA structure. There are numerous reports on the influence of mRNA sequence, in particular the 3′-UTR. For this reason we have kept the same 3′-UTR in the expression plasmids.

Interestingly, IRES elements of different nature and sequence are affected by this negative influence, although to different degrees. This indicates that the inhibitory effect is mediated by a common component(s) of the reinitiation machinery, but one that is not part of the cap-dependent translation machinery.

The EMCV IRES element is the least affected of the three elements tested when the unfavourable Fluc was positioned in the first cistron. This might explain the high frequency of successful use of this IRES element. Interestingly, this IRES element is the only one for which efficient translation *in vitro* has been reported (52).

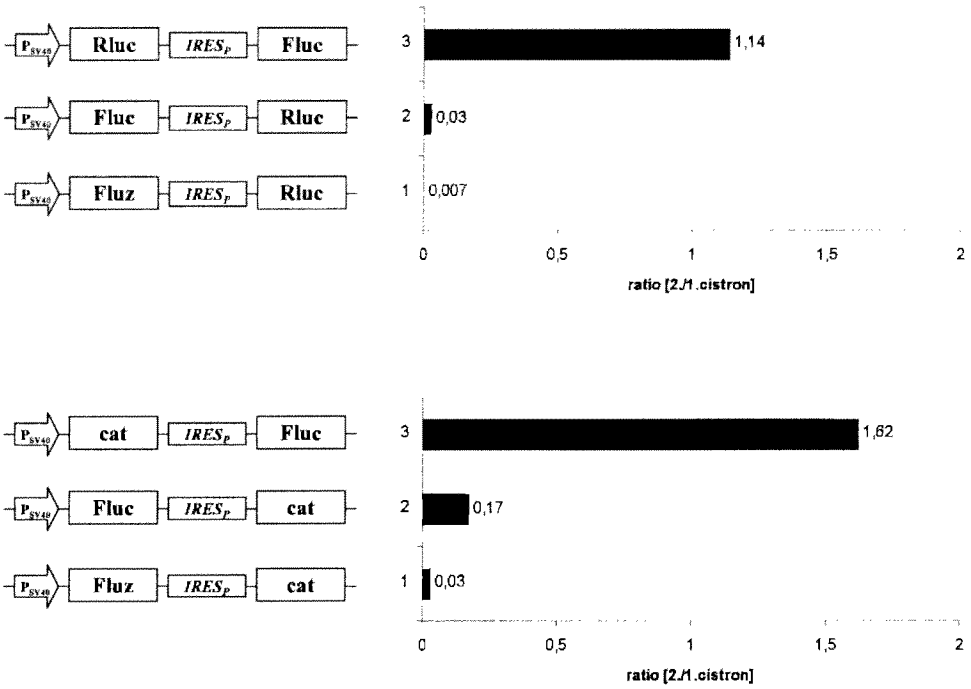

Figure 5. Effect of arrangement of wild-type and mutant firefly luciferase reporter genes on cap-dependent and IRES-dependent translation. A schematic representation of expression constructs used to measure reporter gene expression after transient transfection of C243 cells is shown on the left. Relative expression of wild-type firefly luciferase, *Renilla* luciferase, mutant firefly luciferase (Fluz) and cat from the indicated plasmids was determined. cat values from comparable monocistronic constructs were converted to firefly luciferase analogous values in order to obtain comparable relative expression values. The luciferase values (first cistron) for all six constructs were between 2.4×10^5 and 7×10^5 U/μg.

Neither the translation process *per se* nor the resulting translation products seem to be responsible for the inhibitory activity on IRES-mediated translation. The current data direct us more towards the sequence of the inhibitory cistrons. A comparison of the sequences of HBcAg and firefly luciferase does not show any homology. This does not necessarily exclude a sequence-mediated effect, but effects of secondary structure might be more convincing.

The most intriguing question concerns the fact that the inhibitory activity is only exerted from the first cistron position. Since in our experiments we could not achieve complete inhibition of the first cistron by poliovirus 2A protease we cannot fully exclude an effect of the cap-dependent translation process. However, complete resistance of IRES-mediated translation to partial cap-dependent translation inhibition leads us to believe that it is the presence of a particular sequence or structure which mediates the inhibitory effect. How this is transmitted to the downstream IRES-initiated translation process is not understood.

In summary, our data show that certain cistrons can inhibit the activity of IRES elements of different sequence and category in translational reinitiation. We are still far from a mechanistic understanding of the phenomena described. The above interpretation of the results may not necessarily be valid for other constructs. Nevertheless, with this work we have developed a basis for a more systematic construction of new oligocistronic expression plasmids. The frequent use of IRES elements and the lack of alternatives deserves further examination, with the goal of predictable construction of bi- and oligocistronic vectors.

REFERENCES

1. Sachs,A.B., Sarnow,P. and Hentze,M.W. (1997) Starting at the beginning, middle and end: translation initiation in eukaryotes. *Cell*, **89**, 831–838.
2. Davies,M.V. and Kaufman,R.J. (1992) Internal translation initiation in the design of improved expression vectors. *Curr. Opin. Biotechnol.*, **3**, 512–517.
3. Dirks,W., Wirth,M. and Hauser,H. (1993) Bicistronic transcription units for gene expression in mammalian cells. *Gene*, **128**, 247–249.
4. Mountford,P.S. and Smith,A.G. (1995) Internal ribosome entry sites and dicistronic RNAs in mammalian transgenesis. *Trends Genet.*, **11**, 179–184.
5. Martinez-Salas,E. (1999) Internal ribosome entry site biology and its use in expression vectors. *Curr. Opin. Biotechnol.*, **10**, 458–464.
6. Dirks,W. and Hauser,H. (1994) Equimolar expression of two protein chains in mammalian cells. In Spier,R., Griffiths,B. and Berthold,W. (eds), *Animal Cell Technology: Products of Today, Prospects for Tomorrow*. Butterworths, Oxford, UK, pp. 610–616.
7. Borman,A.M., Bailly,J.L., Girard,M. and Kean,K.M. (1995) Picornavirus internal ribosome entry segments: comparison of translation efficiency and the requirements for optimal internal initiation of translation *in vitro*. *Nucleic Acids Res.*, **23**, 3656–3663.
8. Kirchhoff,S., Köster,M., Wirth,M., Schaper,F., Gossen,M., Bujard,H. and Hauser,H. (1995) Identification of mammalian cell clones exhibiting highly regulated expression from inducible promoters. *Trends Genet.*, **11**, 219–220.
9. Wild,J., Gruner,B., Metzger,K., Kuhrober,A., Pudollek,H.P., Hauser,H., Schirmbeck,R. and Reimann,J. (1998) Polyvalent vaccination against hepatitis B surface and core antigen using a dicistronic expression plasmid. *Vaccine*, **16**, 353–360.

10. Fussenegger,M., Bailey,J., Hauser,H. and Mueller,P.P. (1999) Genetic optimization of recombinant protein production by mammalian cells. *Trends Biotechnol.*, **17**, 43–50.
11. Adam,M.A., Ramesh,N., Miller,A.D. and Osborne,W.R. (1991) Internal initiation of translation in retroviral vectors carrying picornovirus 5′ nontranslated regions. *J. Virol.*, **65**, 4985–4990.
12. Morgan,R.A., Couture,L., Elroy-Stein,O., Ragheb,J., Moss,B. and Anderson,W.F. (1992) Retroviral vectors containing putative internal ribosome entry sites: development of a polycistronic gene transfer system and applications to human gene therapy. *Nucleic Acids Res.*, **20**, 1293–1299.
13. Ramesh,N., Kim,S.T., Wei,M.Q., Khalighi,M. and Osborne,W.R. (1996) High-titer bicistronic retroviral vectors employing foot-and-mouth disease virus internal ribosome entry site. *Nucleic Acids Res.*, **24**, 2697–2700.
14. Verhoeyen,E., Hauser,H. and Wirth,D. (2001) Conversion to expression stability by Flp-mediated cassette replacement. *Hum. Gene Ther.*, **12**, 933–944.
15. Pelletier,J. and Sonenberg,N. (1988) Internal initiation of translation of eukaryotic mRNA directed by a sequence derived from poliovirus RNA. *Nature*, **334**, 320–325.
16. Gan,W. and Rhoads,R.E. (1996) Internal initiation of translation directed by the 5′-untranslated region of the mRNA for eIF4G, a factor involved in the picornavirus-induced switch from cap-dependent to internal initiation. *J. Biol. Chem.*, **271**, 623–626.
17. Vagner,S., Gensac,M.C., Maret,A., Bayard,F., Amalric,F., Prats,H. and Prats,A.C. (1995) Alternative translation of human fibroblast growth factor 2 mRNA occurs by internal entry of ribosomes. *Mol. Cell. Biol.*, **15**, 35–44.
18. Reynolds,J.E., Kaminski,A., Kettinen,H.J., Grace,K., Clarke,B.E., Rowlands,D.J. and Jackson,R.J. (1995) Unique features of internal initiation of translation of hepatitis C virus translation. *EMBO J.*, **14**, 6010–6020.
19. Bernstein,J., Sella,O., Le,S.-Y. and Elroy-Stein,O. (1997) PDGF2/c-sis mRNA leader contains a differentiation linked internal ribosomal entry site (D-IRES). *J. Biol. Chem.*, **272**, 9356–9362.
20. Ye,X.P., Fong,P., Iizuka,N., Choate,D. and Cavener,D.R. (1997) *Ultrabithorax* and *Antennapedia* 5′ untranslated regions promote developmentally regulated internal translation initiation. *Mol. Cell. Biol.*, **17**, 1714–1721.
21. Akiri,G., Nahari,D., Finkelstein,Y., Le,S.Y., Elroy-Stein,O. and Levi,B.-Z. (1998) Regulation of vascular endothelial growth factor (VEGF) expression is mediated by internal initiation of translation and alternative initiation of transcription. *Oncogene*, **17**, 227–236.
22. Kim,J.G., Armstrong,R.C., Berndt,J.A., Kim,N.W. and Hudson,L.D. (1998) A secreted DNA-binding protein that is translated through an internal ribosome entry site (IRES) and distributed in a discrete pattern in the central nervous system. *Mol. Cell. Neurosci.*, **12**, 119–140.
23. Negulescu,D., Leong,L.E.-C., Chandy,K.G., Semler,B.L. and Gutman,G.A. (1998) Translation initiation of cardiac voltage-gated potassium channel by internal ribosome entry. *J. Biol. Chem.*, **273**, 20109–20113.
24. Stein,I., Itin,A., Einat,P., Skaliter,R., Grossman,Z. and Keshet,E. (1998) Translation of vascular endothelial growth factor mRNA by internal ribosome entry: implications for translation under hypoxia. *Mol. Cell. Biol.*, **18**, 3112–3119.
25. Chappell,S.A., Edelman,G.M. and Mauro,V. (2000) A 9-nt segment of a cellular mRNA can function as an internal ribosome entry site (IRES) and when present in linked multiple copies greatly enhances IRES activity. *Proc. Natl Acad. Sci. USA*, **97**, 1536–1541.
26. Henis-Korenblit,S., Strumpf,N.L., Goldstaub,D. and Kimchi,A. (2000) A novel form of DAP5 protein accumulates in apoptotic cells as a result of caspase cleavage and internal ribosome entry site-mediated translation. *Mol. Cell. Biol.*, **20**, 496–506.
27. Jackson,R.J. and Kaminski,A. (1995) Internal initiation of translation in eukaryotes: the picornavirus paradigm and beyond. *RNA*, **1**, 985–1000.
28. Le,S.-Y. and Maizel,J.V. (1997) A common RNA structural motif involved in the internal initiation of translation of cellular mRNAs. *Nucleic Acids Res.*, **25**, 362–369.
29. Belsham,G.J. and Sonenberg,N. (1996) RNA–protein interactions in regulation of picarnovirus RNA translation. *Microbiol. Rev.*, **60**, 499–511.
30. Huez,I., Creancier,L., Audigier,S., Gensac,M.C., Prats,A.C. and Prats,H. (1998) Two independent internal ribosome entry sites are involved in translation initiation of vascular endothelial growth factor mRNA. *Mol. Cell. Biol.*, **18**, 6178–6190.
31. Pestova,T.V., Hellen,C.U.T. and Shatsky,I.N. (1996) Canonical eukaryotic initiation factors determine initiation of translation by internal ribosome entry. *Mol. Cell. Biol.*, **16**, 6859–6869.
32. Roberts,L.O., Seamons,R.A. and Belsham,G.J. (1998) Recognition of picornavirus internal ribosome entry sites within cells; influence of cellular and viral proteins. *RNA*, **4**, 520–529.
33. Borman,A.M., Le Mercier,P., Girard,M. and Kean,K.M. (1997) Comparison of picornaviral-IRES driven internal initiation of translation in cultured cells of different origins. *Nucleic Acids Res.*, **25**, 925–932.
34. Oumard,A., Hennecke,M., Hauser,H. and Nourbakhsh,M. (2000) Translation of NRF mRNA is mediated by highly efficient internal ribosome entry. *Mol. Cell. Biol.*, **20**, 2755–2759.
35. Müller,P., Oumard,A., Wirth,D., Kröger,A. and Hauser,H. (2001) Polyvalent vectors for coexpression of multiple genes. In Schleef,M. (ed.), *Plasmids for Therapy and Vaccination*. Wiley-VCH, Weinheim, Germany, pp. 119–137.
36. Zitvogel,L., Tahara,H., Cai,Q., Storkus,W.J., Muller,G., Wolf,S.F., Gately,M., Robbins,P.D. and Lotze,M.T. (1994) Construction and characterization of retroviral vectors expressing biologically active human interleukin-12. *Hum. Gene Ther.*, **5**, 1493–1506.
37. Fussenegger,M., Mazur,X. and Bailey,J.E. (1998) pTRIDENT, a novel vector family for tricistronic gene expression in mammalian cells. *Biotechnol. Bioeng.*, **57**, 1–10.
38. Mielke,C., Tümmler,M., Schübeler,D., von Hoegen,I. and Hauser,H. (2000) Stabilized, long-term expression of heteromeric proteins from tricistronic mRNA. *Gene*, **254**, 1–8.
39. Sambrook,R. and Russell,D.W. (2001) *Molecular Cloning: A Laboratory Manual*, 3rd Edn. Cold Spring Harbor Laboratory Press, Cold Spring Harbor, NY.
40. Schirmbeck,R., von Kampen,J., Metzger,K., Wild,J., Grüner,B., Schleef,M., Kröger,A., Hauser,H. and Reimann,J. (1999) DNA-based vaccination with polycistronic expression plasmids. *Methods Mol. Med.*, **29**, 313–322.
41. Schirmbeck,R., Wild,J. and Reimann,J. (1998) Similar as well as distinct MHC class I-binding peptides are generated by exogenous and endogenous processing of hepatitis B virus surface antigen. *Eur. J. Immunol.*, **28**, 4149–4161.
42. Ladel,C.H., Flesch,I.E., Arnoldi,J. and Kaufmann,S.H. (1994) Studies with MHC-deficient knock-out mice reveal impact of both MHC I and MHC II-dependent T cell responses in *Listeria monocytogenes* infection. *J. Immunol.*, **153**, 3116–3122.
43. Thoma,S., Bonhagen,K., Vestweber,D., Hamann,A. and Reimann,J. (1998) Expression of selectin-binding epitopes and cytokines by CD4+ T cells repopulating scid mice with colitis. *Eur. J. Immunol.*, **28**, 1785–1795.
44. de Wet,J.R., Wood,K.V., DeLuca,M., Helsinki,D.R. and Subramani,S. (1987) Firefly luciferase gene: structure and expression in mammalian cells. *Mol. Cell. Biol.*, **7**, 725–737.
45. Gorman,C.M., Moffat,L.F. and Howard,B.H. (1982) Recombinant genomes which express chloramphenicol acetyltransferase in mammalian cells. *Mol. Cell. Biol.*, **2**, 1044–1051.
46. Oie,H., Gazdar,A.F., Buckler,C.E. and Baron,S. (1977) High interferon producing line of transformed murine cells *J. Gen. Virol.*, **1**, 107–109.
47. Dirks,W., Mielke,C., Karreman,S., Haase,B., Wirth,M., Lindenmaier,W. and Hauser,H. (1994) Applications of expression vectors containing bicistronic transcription units in mammalian cells. In Fusenig,N.E. and Graf,H. (eds), *Cell Culture in Pharmaceutical Research*. Springer Verlag, Heidelberg, Germany, pp. 239–266.
48. Ross,J. (1995) mRNA stability in mammalian cells. *Microbiol. Rev.*, **59**, 423–450.
49. Day,D.A. and Tuite,M.F. (1998) Post-transcriptional gene regulatory mechanisms in eukaryotes: an overview. *Endocrinology*, **157**, 361–371.
50. Attal,J., Theron,M.C. and Houdebine,L.M. (1999) The optimal use of IRES (internal ribosome entry site) in expression vectors. *Genet. Anal.*, **15**, 161–165.
51. Rees,S., Coote,J., Stables,J., Goodson,S., Harris,S. and Lee,M.G. (1996) Bicistronic vector for the creation of stable mammalian cell lines that predisposes all antibiotics-resistant cells to express recombinant protein. *Biotechniques*, **20**, 48–56.
52. Jang,S.K., Krausslich,H.G., Nicklin,M.J., Duke,G.M., Palmenberg,A.C. and Wimmer,E. (1988) A segment of the 5′ nontranslated region of encephalomyocarditis virus RNA directs internal entry of ribosomes during *in vitro* translation. *J. Virol.*, **62**, 2636–2643.

THE JOURNAL OF BIOLOGICAL CHEMISTRY VOL. 281, NO. 49, pp. 38069–38080, December 8, 2006

Physical and Functional Interaction of the p14^{ARF} Tumor Suppressor with Ribosomes*

Received for publication, October 5, 2006 Published, JBC Papers in Press, October 11, 2006, DOI 10.1074/jbc.M609405200

Helen Rizos[‡1], Heather A. McKenzie[‡], Ana Luisa Ayub[‡], Sarah Woodruff[‡], Therese M. Becker[‡], Lyndee L. Scurr[‡2], Joachim Stahl[§], and Richard F. Kefford[‡]

From the [‡]Westmead Institute for Cancer Research, University of Sydney at Westmead Millennium Institute, Westmead Hospital, Westmead, New South Wales 2145, Australia and the [§]Max-Delbrück-Centrum für Molekulare Medizin, Robert-Rössle-Strasse 10, D-13125 Berlin-Buch, Germany

Alterations in the p14^{ARF} tumor suppressor are frequent in many human cancers and are associated with susceptibility to melanoma, pancreatic cancer, and nervous system tumors. In addition to its p53-regulatory functions, p14^{ARF} has been shown to influence ribosome biogenesis and to regulate the endoribonuclease B23, but there remains considerable controversy about its nucleolar role. We sought to clarify the activities of p14^{ARF} by studying its interaction with ribosomes. We show that p14^{ARF} and B23 interact within the nucleolar 60 S preribosomal particle and that this interaction does not require rRNA. In contrast to previous reports, we found that expression of p14^{ARF} does not significantly alter ribosome biogenesis but inhibits polysome formation and protein translation *in vivo*. These results suggest a ribosome-dependent p14^{ARF} pathway that regulates cell growth and thus complements p53-dependent p14^{ARF} functions.

The *INK4a/ARF* locus on chromosome 9 is frequently altered in human cancer, and inherited *INK4a/ARF* mutations are associated with melanoma susceptibility in 20–40% of multiple case melanoma families (1). This complex sequence encodes the melanoma tumor suppressor proteins, p16^{INK4a} and p14^{ARF} from alternative spliced transcripts in different reading frames (2, 3). Both proteins are centrally involved in the regulation of cell cycle and apoptotic programs in response to oncogenic stimuli and are therefore frequently targeted in tumor development and progression (4). *INK4a/ARF*-deficient mice are tumor-prone (5–7), and those with melanocyte-specific expression of activated H-*ras* develop cutaneous melanomas with high penetrance (8). High density mapping on chromosome 9p in human melanomas has identified *p14^{ARF}* as the most commonly deleted *INK4a/ARF* gene (9), and individuals with altered ARF, but apparently wild type p16^{INK4a}, are melanoma-prone (10–13).

p14^{ARF} interacts with the p53 negative regulator hdm2, and inhibits its p53-specific E3[3] ubiquitin ligase activity (14–17). It has been proposed that ARF physically sequesters hdm2 in nucleoli, thus relieving nucleoplasmic p53 from hdm2-mediated degradation (18). Recent data, however, suggest that nucleolar relocalization of hdm2 is not required for p53 activation (19) and that the redistribution of ARF into the nucleoplasm enhances its interaction with hdm2 and its p53-dependent growth-suppressive activity (20, 21). Accordingly, increasing nucleolar localization of ARF reduces ARF p53-dependent functions and diminishes ARF-hdm2 complex formation (21). This current model of ARF function supports the concept that nucleolar disruption contributes to p53 signaling (22) because many stress signals perturb the nucleolus, causing the release of nucleolar proteins (including ARF, L11, L23, L5, and B23) that activate the p53 pathway (23–27).

Nucleolar ARF, rather than residing in inactive "storage" (20, 21, 28), may regulate ribosome biogenesis by retarding the processing of early 47 S/45 S and 32 S rRNA precursors (29). These effects do not depend on hdm2 or p53 but may involve the interaction of ARF with nucleophosmin/B23 in complexes of very high molecular mass (30, 31). B23 is an abundant nucleolar endoribonuclease that is required for the nucleolar targeting of ARF (21) and for the maturation of 28S rRNA (32). Consistent with its role in inhibiting rRNA processing, ARF promotes the ubiquitination and degradation of B23 (31).

Because melanoma-associated ARF mutants have altered nucleolar localization (11) and ARF can mobilize out of the nucleolus in response to stress signals (14, 33), we sought to refine the functional role of p14^{ARF}. We now show that endogenous p14^{ARF} and B23 fractionate with the nucleolar 60 S preribosomal particle. Moreover, p14^{ARF} and B23 interact within the 60 S complex in a rRNA-independent manner. p14^{ARF} does not significantly alter the amount of nuclear preribosomal particles but inhibits polysome formation and retards protein translation. We propose that the p14^{ARF} tumor suppressor functions to integrate cell growth and cell cycle progression with nucleolar ARF regulating ribosome function, whereas nucleoplasmic ARF responds to cellular stress by activating p53-dependent growth arrest.

* This work was supported by the National Health and Medical Research Council, the University of Sydney, and the New South Wales Health Department. The costs of publication of this article were defrayed in part by the payment of page charges. This article must therefore be hereby marked "*advertisement*" in accordance with 18 U.S.C. Section 1734 solely to indicate this fact.

[1] National Health and Medical Research Council RD Wright Fellow, University of Sydney. To whom correspondence should be addressed: Westmead Inst. for Cancer Research, University of Sydney at Westmead Millennium Institute, Westmead Hospital, Westmead NSW 2145, Australia. Tel.: 61-2-9845-9509; Fax: 61-2-9845-9102; E-mail: helen_rizos@wmi.usyd.edu.au.

[2] Cameron Melanoma Research Fellow, Melanoma and Skin Cancer Research Institute, University of Sydney.

[3] The abbreviations used are: E3, ubiquitin-protein isopeptide ligase; IPTG, sopropyl β-D-thiogalactopyranoside; eIF, eukaryotic initiation factor.

EXPERIMENTAL PROCEDURES

Cell Culture—Human U2OS osteosarcoma cells (ARF-null, p53 wild type), Saos 2 osteosarcoma cells (ARF wild type, p53-null) and WMM1175 melanoma cells (ARF-null, p53-null (34)) were grown in Dulbecco's modified Eagle's medium (Trace Scientific, Sydney, Australia) supplemented with 10% fetal bovine serum and glutamine. All of the cells were cultured in a 37 °C incubator with 5% CO_2.

The U2OS_ARF, WMM1175_ARF, or WMM1175_$p16^{INK4a}$ cell clones carrying the stably integrated $p14^{ARF}$ gene or $p16^{INK4a}$ gene under IPTG-inducible expression control have been described previously (35, 36). The NARF2-E6 cells were initially provided by Dr. Gordon Peters (Cancer Research UK London Research) and have been described elsewhere (28). Briefly, these cells express an IPTG-inducible form of human $p14^{ARF}$ and constitutively accumulate human papillomavirus E6 protein, which promotes p53 degradation. Stable cell clones were seeded 24 h prior to induction in the absence of antibiotics and were induced with 1–5 mM IPTG.

Western Blotting—Total cellular proteins were extracted for 1 h at 4 °C using radioimmune precipitation assay lysis buffer containing protease inhibitors (Roche Applied Science). Proteins (30–50 μg) were resolved on 12% SDS-polyacrylamide gels and transferred to Immobilon-P membranes (Millipore). Western blots were probed with antibodies against p53 (DO-1; Santa Cruz), $p21^{Waf1}$ (C-19; Santa Cruz), $p14^{ARF}$ (DCS-240; Sigma), E2F-1 (C-20; Santa Cruz), B23 (C19; Santa Cruz), L28 (A16; Santa Cruz), topoisomerase II (Oncogene Research), tubulin (Molecular Probes), actin (AC-74; Sigma), and eIF2α (Cell Signaling). Antibodies against S6, S7, and L37 were prepared according to Ref. 37.

Indirect Immunofluorescence—Cultured cells (1×10^5) seeded on coverslips in six-well plates were washed in phosphate-buffered saline and fixed in 3.7% formaldehyde. The cells were immunostained for 50 min with primary antibodies followed by a 50-min exposure to Texas Red- or FITC-conjugated secondary IgG (Sigma).

Cell Cycle Analysis—The cells were fixed in 70% ethanol at 4 °C for at least 1 h, washed in phosphate-buffered saline, and stained with propidium iodide (50 ng/μl) containing RNase A (50 ng/μl). DNA content from at least 2000 cells was analyzed using ModFIT software.

Sucrose Density Gradient Fractionation—Cytoplasmic ribosomes were isolated as previously described (38), except that the lysis buffer contained only 0.2% Nonidet P-40. The lysates were centrifuged at 10,000 rpm for 10 min, and postmitochondrial supernatant was usually layered on 10–45% or 10–25% (w/w) sucrose density gradients in 10 mM Tris-HCl, pH 7.2, 60 mM KCl, 10 mM $MgCl_2$, 1 mM dithiothreitol, 0.1 mg of heparin/ml. To disrupt the 80 S cytoplasmic ribosome, $MgCl_2$ was omitted during lysis, and the lysates were separated in 5–25% (w/w) sucrose gradients in 10 mM Tris-HCl, pH 7.2, 60 mM KCl, 1 mM EDTA, 1 mM dithiothreitol, 0.1 mg of heparin/ml. The gradients were centrifuged at 36,000 rpm for 2 h 40 min at 5 °C in a Beckman SW41Ti rotor and fractionated through a Bio-Rad EM-1 UV monitor for continuous measurement of the absorbance at 254 nm.

Isolation of nuclear extracts was performed as described (38). Nuclear proteins (1–1.5 mg) were overlaid on 15–30% (w/w) sucrose gradients in 25 mM Tris, pH 7.5, 100 mM KCl, 1 mM dithiothreitol, 2 mM EDTA and centrifuged at 38,000 rpm for 3 h 20 min at 5 °C in a Beckman SW41Ti rotor. Where indicated, the nuclear extract was treated with RNase A (100 μg/ml) for 10 min at room temperature. The gradients were analyzed as above. The proteins were precipitated from the fractions with trichloroacetic acid prior to Western blotting, and RNA was extracted from fractions using TRI-reagent LS (Sigma).

Immunoprecipitations—For immunoprecipitation analysis, U20S_ARF cells were left untreated or exposed to 1 mM IPTG for up to 96 h. Nuclear protein extracts (1.5 mg) were fractionated on sucrose gradients as detailed previously. Immunoprecipitations were performed overnight using 1 μg of antibody chemically adsorbed to M450-tosylactivated DYNALbeads (DYNAL) as described by the manufacturer. Immunoprecipitates were washed four times with NET2 (50 mM Tris-HCl, pH 7.5, 150 mM NaCl, 0.05% Nonidet P-40 containing protease inhibitors (Roche Applied Science)) lysis buffer, resolved using SDS-PAGE, and detected by immunoblot analysis. Extraction of RNA post-immunoprecipitation was performed using TRI-reagent LS (Sigma).

Transcription Analysis—To measure RNA polymerase I transcription after $p14^{ARF}$ expression, U20S_ARF cells were induced with 1 mM IPTG for 72 h. The cells were permeabilized on ice in 20 mM Tris-HCl, pH 7.4, 5 mM $MgCl_2$, 25% glycerol, 0.5 mM EGTA, 0.5 mM phenylmethylsulfonyl fluoride, 25 units of RNaseOUT (Invitrogen), and 0.05% Triton X-100. After permeabilization, the cells were resuspended in transcription buffer (50 mM Tris-HCl, pH 7.4, 10 mM $MgCl_2$, 150 mM NaCl, 25% glycerol, 0.5 mM phenylmethylsulfonyl fluoride, 25 units of RNaseOUT (Invitrogen), 0.5 mM ATP/CTP/GTP (Promega), and 0.5 mM bromouridine (Sigma)), and run-on transcription was performed at room temperature for 30 min. The cells were fixed and immunostained as detailed above.

Analysis of RNA Processing—Mammalian cells (2×10^5) were starved for 30 min in methionine-free medium, labeled for 30 min with 50 μCi/ml [methyl-^{3}H]methionine (85 Ci/mmol; Amersham Biosciences), and chased in medium containing excess unlabeled methionine. RNA was extracted with TRI-reagent (Sigma) and analyzed essentially as described (29).

Biochemical Fractionation—Cultured cells were permeabilized in buffer A (10 mM HEPES, pH 7.9, 15 mM KCl, 2 mM $MgCl_2$, 0.1 mM EDTA, and protease inhibitors (Roche Applied Science)) for 10 min and then supplemented with 0.2% Nonidet P-40. The cytosol fraction was collected, and the cells were washed in buffer A prior to solubilization using equal volumes of buffer B (50 mM HEPES, pH 7.9, 50 mM KCl, 0.1 mM EDTA, and protease inhibitors) and buffer C (50 mM HEPES, pH 7.9, 0.8 M KCl, 0.1 mM EDTA, and protease inhibitors). The soluble nuclear fractions were collected after centrifugation. Soluble nuclear and cytosolic fractions derived from equal cell numbers were analyzed by immunoblotting.

Protein Synthesis Measurements—The cells (1×10^4) were plated in methionine-free, Dulbecco's modified Eagle's medium in 96-well FLASH plates (PerkinElmer Life Sciences). Approximately 24 h post-seeding, the medium was replaced

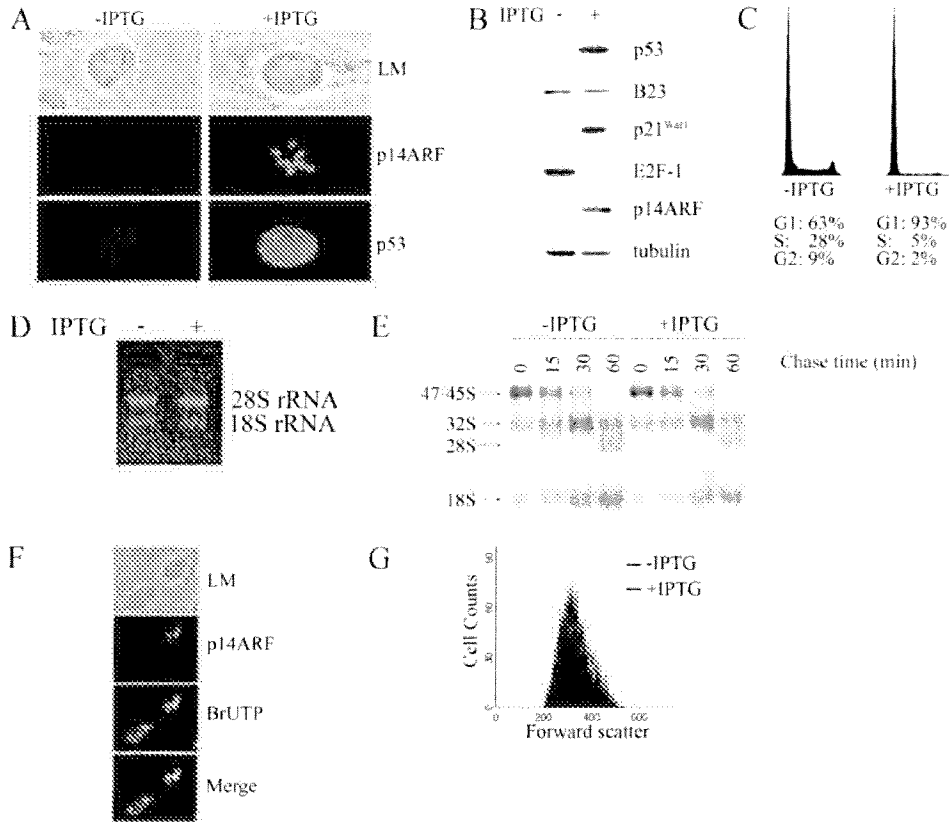

FIGURE 1. **Accumulation of $p14^{ARF}$ in U20S_ARF cells promotes p53 accumulation and cell cycle arrest but no detectable changes in rRNA synthesis or cell size.** U20S_ARF cells were treated with 1 mM IPTG (+) or left untreated (−) for 72 h, unless otherwise indicated. *A*, the subcellular distribution of $p14^{ARF}$ and p53 was analyzed by immunofluorescence. *LM*, light microscopy. *B*, total proteins extracted from IPTG-treated or untreated cells were separated using SDS-PAGE and immunoblotted for the indicated proteins. *C*, the cell cycle distribution of induced and uninduced U20S_ARF was determined using propidium iodide staining. *D*, total RNA extracted from equal numbers of U20S_ARF cells was separated on a formaldehyde-containing agarose gel and visualized by ethidium bromide staining. *E*, following IPTG treatment (24 h), RNA was pulse labeled with [methyl-^{3}H]methionine for 30 min and chased in nonradioactive medium for the times indicated. Eight thousand ^{3}H cpm were resolved on agarose gel, transferred to a membrane, and visualized by fluorography. Positions of rRNAs and precursors are indicated on the *left*. *F*, permeabilized U20S_ARF cells, induced with 1 mM IPTG and showing a $p14^{ARF}$ positive and negative cell, were pulse-labeled with bromouridine for 30 min before fixation to determine location of $p14^{ARF}$ and ongoing RNA transcription. *G*, flow cytometric forward scatter profiles of uninduced and induced U20S_ARF cells.

with methionine-free Dulbecco's modified Eagle's medium containing [^{3}H]methionine at 10 μCi/ml, and protein synthesis was measured 72 h later using a TopCount luminometer (Packard).

RESULTS

Impact of Induced $p14^{ARF}$ Expression—To evaluate the influence of $p14^{ARF}$ accumulation on cell proliferation, the U20S osteosarcoma cell line, which is wild type for both p53 and pRb (39), was engineered to express wild type $p14^{ARF}$. In this U20S_ARF cell line, $p14^{ARF}$ expression was induced with 1 mM IPTG. Three days post-induction these cells behaved as expected, with strong nucleolar expression of $p14^{ARF}$ (Fig. 1, *A* and *B*), increased p53 levels, increased expression of the p53-transcriptional target $p21^{Waf1}$, decreased levels of the transcription factor E2F-1 (40) (Fig. 1*B*), and potent G_1 phase cell cycle arrest (Fig. 1*C*). In addition, although $p14^{ARF}$ has been reported to induce the degradation of B23 (31) and inhibit rRNA processing (29) (which would limit the production of mature rRNAs), we found that the presence of $p14^{ARF}$ had no detectable effect on the accumulation of B23 (Fig. 1*B*), on the steady-state levels or processing of mature 28 and 18 S rRNA species (Fig. 1, *D* and *E*), on nucleolar transcription activity when RNA polymerase I transcription was visualized by pulse labeling with bromouridine and immunostaining with anti-bromodeoxyuridine antibody (Fig. 1*F*), or on cell size (Fig. 1*G*).

$p14^{ARF}$ Associates with the 60 S Preribosomal Particles—The association of tandem affinity purification-tagged murine $p19^{ARF}$ with ribosomal proteins and the fractionation of $p19^{ARF}$ in large nuclear multiprotein complexes (2–5 MDa) (30) suggested that the ARF protein associates with preribosomal particles within the nucleolus. To examine this possibility, nuclear extracts derived from Saos 2 osteosarcoma cells, which express endogenous $p14^{ARF}$, were subjected to sucrose gradient centrifugation to separate preribosomal particles. Under these conditions three detectable peaks were resolved, and assignment of 40 and 60 S preribosomal subunits was confirmed by resolving the extracted RNA species and Western immunoblotting for ribosomal proteins, including antibodies of the small ribosomal subunit, S7 and the large ribosomal subunit, L28, and L37. Western blot detection of endogenous $p14^{ARF}$ in Saos 2 cells confirmed that the majority of $p14^{ARF}$ cosedimented with the 60 S preribosome particles (Fig. 2*A*). Likewise, sucrose density gradient ultracentrifugation of IPTG-treated U20S_ARF nuclear cell extracts followed by Western immunodetection confirmed that a large proportion of the induced $p14^{ARF}$ cosedimented with the 60 S preribosome particles (Fig. 2, *B* and *C*).

To verify that $p14^{ARF}$ is a component of preribosomes, nuclear Saos 2 extracts were either left untreated or treated with RNase A before being subjected to fractionation on a sucrose gradient. As expected, treatment with RNase A disrupted ribosomal particles and resulted in the loss of preribosome peaks, and ribosomal protein S7, B23, and $p14^{ARF}$ remained at the top of the sucrose gradient (Fig. 2*D*).

$p14^{ARF}$ Interacts with B23 in the 60 S Preribosome Particles—To investigate whether $p14^{ARF}$ is bound to known binding partners within preribosomes, we examined the sedimentation behavior of hdm2, p53, and B23. As shown in Fig. 2, a significant pool of B23 cosedimented with $p14^{ARF}$ within the 60 S preribo-

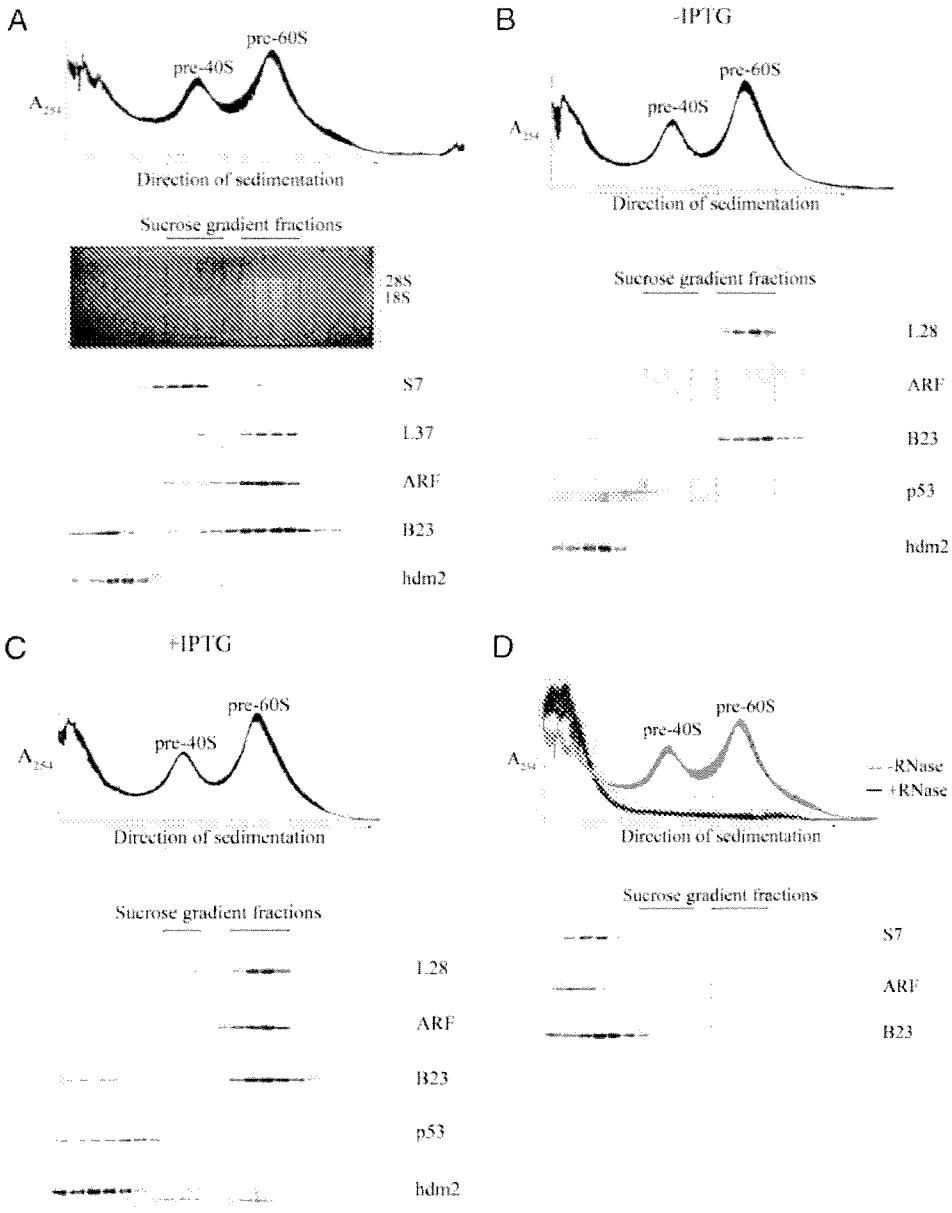

FIGURE 2. **p14ARF fractionates with 60 S preribosomes.** *A*, nuclear extracts of Saos 2 cells were fractionated on 10–30% sucrose density gradients with continuous monitoring of absorbance at 254 nm (*top panel*). RNA extracted from each fraction was resolved by electrophoresis on a formaldehyde-containing agarose gel to demonstrate the sedimentation of the 28 and 18 S rRNA species (*middle panel*). Individual sucrose fractions were precipitated and analyzed by immunoblotting (*bottom panel*). *B*, the inducible U20S_ARF cell line was grown in the absence (−) of IPTG for 48 h. Preribosomes were fractionated and analyzed as detailed above. *C*, the inducible U20S_ARF cell line was grown in the presence (+) of IPTG for 48 h. Preribosomes were fractionated and analyzed as detailed above. *D*, nuclear Saos 2 extracts were either treated with RNase A or left untreated and analyzed as detailed above.

some in both Saos 2 and induced U20S_ARF cells. It is worth noting that B23 also cosedimented with the 60 S preribosomal particles in the absence of p14ARF (Fig. 2*B*). In contrast, hdm2 and its ubiquitination target, p53 were restricted to smaller molecular weight complexes near the top of the sucrose gradients, and this sedimentation behavior was not altered by p14ARF (Fig. 2, *B* and *C*).

Considering that B23 and p14ARF cosediment with the pre-60 S particle, we investigated whether these proteins are complexed within the preribosome. Nuclear extracts derived from IPTG-induced and uninduced U20S_ARF cells were separated using sucrose gradient fractionation. The fractions corresponding to the top of the column (containing small molecular weight complexes), the 40 S preribosome, and the 60 S preribosome were collected. The sucrose fractions (top, 40 and 60 S) were precipitated with antibodies to p14ARF, and recovered immune complexes were denatured, separated on polyacrylamide gels and blotted with antibodies to B23, hdm2, and p53. As expected, the preribosomal fraction of p14ARF was found complexed to B23 (Fig. 3*A*, *lower panel*) and not bound to hdm2 or p53 (data not shown).

We next examined whether the ARF-B23 interaction within the preribosome particles occurs independently of rRNA, because both proteins bind the 5.8 S rRNA found in the 60 S ribosome (29, 30). Expression of p14ARF was induced in U20S_ARF cells with 1 mM IPTG for 96 h, and nuclear extracts were prepared and separated using sucrose density centrifugation. The fractions corresponding to the 60 S preribosome were collected and treated with RNase A. Extraction of the 60 S fraction post-immunoprecipitation with the RNA isolation reagent TRI-Reagent LS confirmed that no detectable RNA was present in the RNase A-treated 60 S preribosomal fractions (Fig. 3*B*, *upper panel*). In the absence of RNA, endogenous B23 was still found in association with p14ARF in the 60 S preribosomal fraction (Fig. 3*B*, *lower panel*).

p14ARF Expression Does Not Influence Preribosome Production—To examine the influence of p14ARF accumulation on nucleolar ribosome assembly, U20S_ARF cells were grown in the absence or presence of 1 mM IPTG for up to 96 h. Equal amounts of nuclear proteins were separated on 15–30% sucrose density gradients. Analysis of 40 and 60 S preribosomal particles revealed no significant changes in the ratio of 60 to 40 S preribosomes subunits at 48, 72, and 96 h post-induction (Fig. 2, *A* and *B*). In particular, the peak height ratio of 60 to 40 S subunits in untreated and treated U20S_ARF cells, 96 h post-induction, was estimated to be 1.6 ± 0.1 and 1.6 ± 0.1, respectively (the means of three independent experiments).

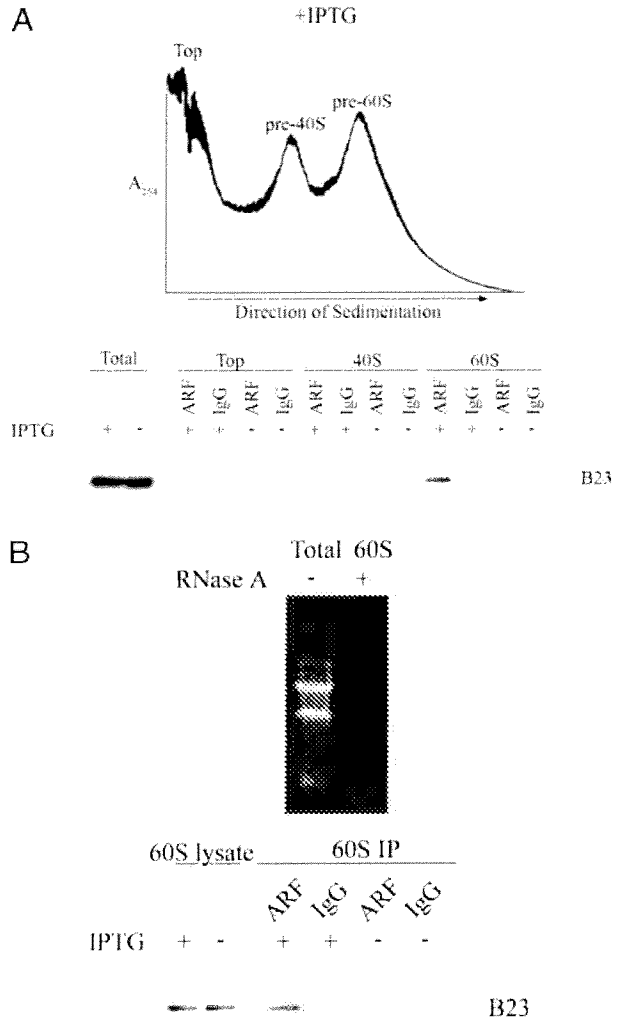

FIGURE 3. **p14ARF and B23 interact and associate with 60 S preribosomes.** *A*, U20S_ARF cells were grown in the presence or absence of 1 mM IPTG for 48 h, and preribosomes were fractionated on 10–30% sucrose density gradients (*upper panel*, induced U20S_ARF fractionation shown). Fractions corresponding to small molecular weight complexes (top of gradient), 40 S preribosomes and 60 S preribosomes were immunoprecipitated with a monoclonal ARF or isotype-matched antibody (IgG). The immunoprecipitates were analyzed for the presence of B23 by Western blotting (*lower panel*). *B*, sucrose gradient fractions corresponding to 60 S preribosomes derived from IPTG-induced and uninduced U20S_ARF cells were treated with RNase A for 30 min at room temperature. The treated fractions were immunoprecipitated with a monoclonal ARF or isotype-matched antibody (IgG). To confirm that rRNA was effectively degraded by RNase treatment, the post-immunoprecipitation lysates were extracted using TRI-reagent LS. Extracted RNA and total cell RNA were resolved in a formaldehyde-containing agarose gel and stained with ethidium bromide (*upper panel*). Immunoprecipitates (*IP*) were analyzed for the presence of B23 by Western blotting (*lower panel*).

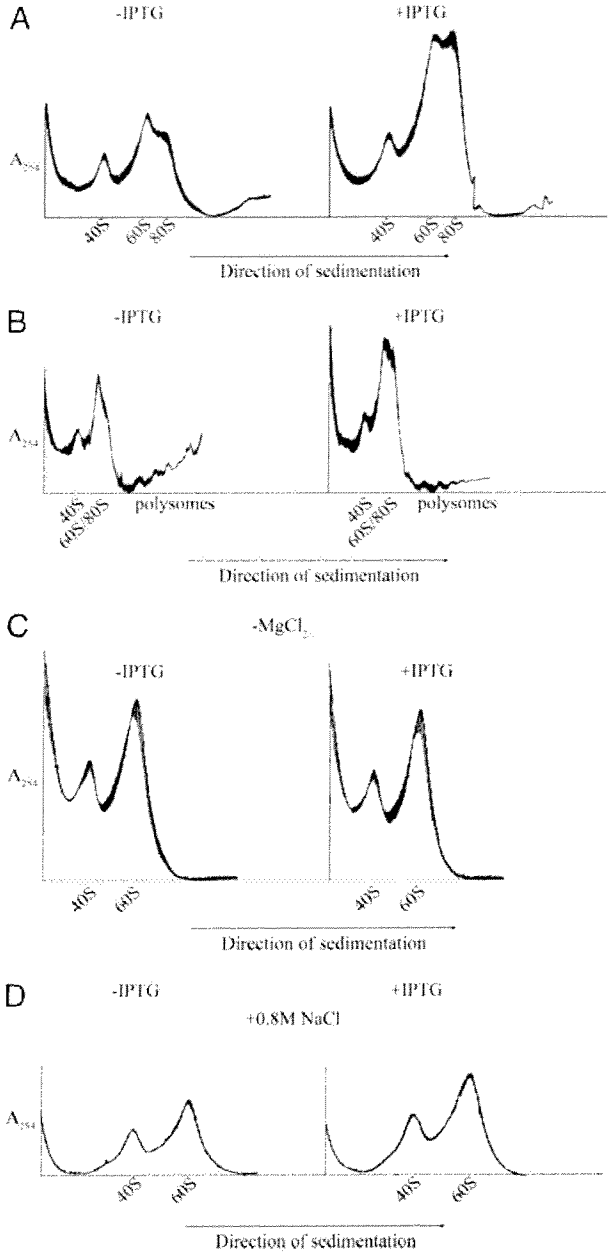

FIGURE 4. **Expression of p14ARF increases formation of inactive 80 S monosomes and reduces polysome formation.** U20S_ARF cells were grown in the presence (+) or absence (−) of 1 mM IPTG for 72 h. *A*, cytoplasmic ribosomes were fractionated on 10–25% sucrose density gradients, to separate monosomes and analyzed with continuous monitoring of absorbance at 254 nm. *B*, cytoplasmic ribosomes were fractionated on 10–45% sucrose density gradients to allow for polysome separation and analyzed with continuous monitoring of absorbance at 254 nm. *C*, cytoplasmic lysates derived from induced and uninduced U20S_ARF cells were prepared in the absence of $MgCl_2$ to separate 80 S ribosomes into their 40 and 60 S subunits. The ribosomes were fractionated on 5–25% sucrose density gradients with continuous monitoring of absorbance at 254 nm. *D*, cytoplasmic lysates derived from induced and uninduced U20S_ARF cells were prepared in the presence of 0.8 M NaCl to dissociate 80 S couples, which consist of 40 and 60 S subunits joined in the absence of mRNA. The ribosomes were fractionated on 10–20% sucrose density gradients with continuous monitoring of absorbance at 254 nm.

p14ARF Expression Inhibits Translation Initiation—The association of p14ARF with preribosomal particles suggested that this tumor suppressor protein might influence cytoplasmic ribosome assembly and/or function. When equal numbers of U20S_ARF cells were extracted and the cytoplasmic lysates separated on 10–25% (to focus on monosome particles) or 10–45% (allows polysome separation) sucrose density gradients, a shift in the distribution of ribosomes to smaller polysomes and larger pools of 80 S monosomes was consistently observed (Fig. 4, *A* and *B*). To determine whether the ARF-induced increase in monosome 80S particles was due to reduced polysome levels, we separated all 80 S subunits, including polysomes, into their 40 and 60 S components by preparing

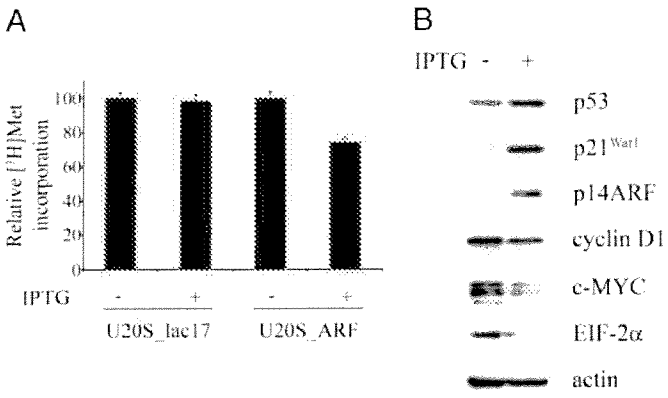

FIGURE 5. **Expression of p14^{ARF} decreases protein synthesis.** *A*, incorporation of [^{3}H] methionine in the U20S_lac17 and U20S_ARF and cells left untreated or exposed to 1 mM IPTG for 72 h. Protein synthesis was measured in FLASH plates using a TopCount luminometer. *B*, total proteins extracted from IPTG-treated (72 h) or untreated cells were separated using SDS-PAGE and immunoblotted for the indicated proteins.

cytoplasmic lysates in the absence of $MgCl_2$. The disruption of 80 S ribosomes resulted in similar levels of 40 and 60 S subunits in the induced and uninduced U20S_ARF cells (Fig. 4*C*). Thus, p14^{ARF} did not alter the accumulation of 40 and 60 S ribosome subunits within the cytoplasm but altered the complexes that they produced. In particular, p14^{ARF} expression caused a significant increase in the proportion of monomeric 80 S subunits (Fig. 4*A*). This was accompanied by a significant reduction in protein translation; U20S_ARF cells induced to express p14^{ARF} for ~72 h incorporated 26 ± 2% less [^{3}H]methionine than the uninduced control cells (Fig. 5*A*). Further, these ARF-expressing cells accumulated less of the translationally regulated c-Myc and cyclin D1 proteins (41) (Fig. 5*B*).

The rate of synthesis of any given protein is determined primarily by the level of translation initiation, and the increase in monosome 80 S subunits in p14^{ARF}-expressing cells was indicative of a block in the initiation phase of translation. The appearance of a large population of nontranslating 80 S couples, consisting of 40 and 60 S subunits joined in the absence of mRNA, is typical of an initiation defect. High levels of salt can readily dissociate these inactive 80 S particles (42), and we examined the effect of including 0.8 M NaCl in the sucrose gradient. As expected, dissociation of inactive couples led to an increase in the levels of cytoplasmic 40 and 60 S ribosome subunits in the p14^{ARF}-expressing U20S_ARF cells. Thus, inactive 80S monosomes are dramatically increased in the presence of p14^{ARF} (Fig. 4*A*) and constitute a major proportion of the ribosome population in the ARF-expressing cells (Fig. 4*D*).

To gain some insight into the mechanism of this translation defect, the accumulation of α-subunit of the eukaryotic initiation factor 2 (eIF2) was examined. eIF2 facilitates binding of the initiator tRNA to the 40 S subunit during translation initiation. Translation can be inhibited by the rapid phosphorylation of the α-subunit (reviewed in Ref. 43), by limiting its expression and accumulation (44), or by specific caspase-mediated eIF2α cleavage during apoptosis (45). Further, phosphorylation of eIFα has been associated with an increase in the formation of monosome 80 S subunits (46). In this study we found that ARF-expressing U20S cells showed a marked reduction in the accumulation of the eIF2α subunit (Fig. 5*B*).

The observed changes in cytoplasmic ribosomes, in particular the increase in the monomers, was not an artifact of IPTG exposure, because addition of IPTG to the parental U20S_lac17 cell line, which expresses the lac repressor, did not alter the ribosomal subunit profile (data not shown). To investigate whether p14^{ARF}-induced effects on polysome production were a result of cell cycle arrest and p53-dependent, we utilized the WMM1175_ARF melanoma and NARF2-E6 osteosarcoma cell lines. Both cell lines express an IPTG-inducible form of p14^{ARF} but are functionally null for p53 function (Fig. 6*A*). The induction of p14^{ARF} in the WMM1175_ARF and NARF2-E6 cells did not induce growth arrest (Fig. 6*A*) but did promote an increase in 80 S monomeric ribosomes and a reduction in polysomes (Fig. 6, *B* and *C*). This ARF-associated decrease in the polysome formation in the WMM1175_ARF cell line is substantial, considering that only 40% of the WMM1175_ARF cells express detectable levels of ARF upon IPTG induction.

To further examine the relationship between cell cycle arrest and inhibition of polysome production, we promoted G_1 cell cycle arrest in the WMM1175_p16^{INK4a} cell line by inducing the expression of the cyclin-dependent kinase inhibitor p16^{INK4a} with 5 mM IPTG for 72 h (36). Although, p16^{INK4a} expression induced potent G_1 cell cycle arrest (Fig. 7*A*), it led to an increase in cell size (Fig. 7*B*) that was accompanied by an increase in the level of cytoplasmic ribosomes and polysome production (Fig. 7*C*).

Considering that p14^{ARF} reduced cytoplasmic ribosome function, we also examined whether p14^{ARF} cosedimented with ribosomes within the nucleolus and cytoplasm. We found that the majority of p14^{ARF} in Saos 2 cells and induced U20S_ARF cells occurred in the nuclear fraction, with no detectable cytoplasmic p14^{ARF} component (Fig. 8).

DISCUSSION

The ARF tumor suppressor plays a central role in limiting cell cycle progression in response to hyperproliferative signals. Cells exposed to oncogenes, such as E2F-1, Ras, or Myc (47–49), accumulate nucleolar ARF, and yet its core function of stabilizing p53 requires its association with hdm2 in the nucleoplasm (21). In this study we sought to explore the interaction of ARF with the nucleolus and have shown that p14^{ARF} is a component of the 60 S preribosome, where it interacts with B23 independently of rRNA. The association of B23 with the 60 S particle is not unexpected, because this protein binds the 28 S rRNA, a major component of the pre-60 S ribosome (50). We also found that ARF did not influence the production of the preribosomes or the steady-state levels of cytoplasmic ribosome subunits but inhibited ribosome function. The impact of p14^{ARF} on ribosome activity may involve the translation initiation factor eIF2α; ARF-expressing U20S cells accumulated low levels of this subunit. Reduced expression of eIF2α in quiescent cells correlates with low levels of protein synthesis (44), whereas induction of eIF2α expression via oncogenes such as c-Myc contributes to the pronounced stimulation of protein production (51). eIF2α is also involved in neoplastic transformation when its function is up-regulated (reviewed in Ref. 52). We are currently investigating whether repression of eIF2α in response to p14^{ARF} expression involves the c-Myc transcrip-

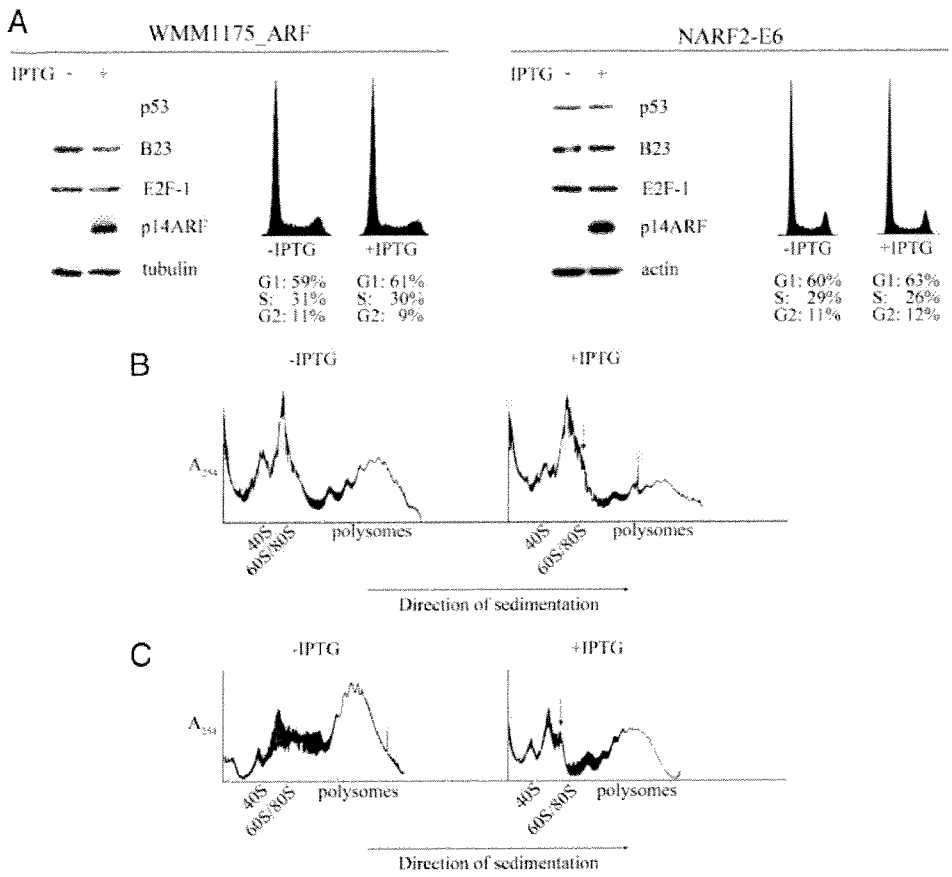

FIGURE 6. **p14ARF reduces polysome formation in a p53-indpendent manner.** The inducible p53-null WMM1175_ARF and NARF2-E6 cell lines were grown in the presence (+) or absence (−) of IPTG for 72 h. *A*, cell lysates were separated on 12% SDS-polyacrylamide gels and immunoblotted for the indicated proteins. Cell cycle distribution of cells either untreated or treated for 72 h with IPTG using propidium iodide staining. *B*, cytoplasmic ribosomes were fractionated on 10–45% sucrose density gradients for the WMM1175_ARF cells with continuous monitoring of absorbance at 254 nm. *C*, cytoplasmic ribosomes were fractionated on 15–45% sucrose density gradients for the NARF2-E6 cells with continuous monitoring of absorbance at 254 nm. The *vertical arrows* indicate the 80 S monomer peaks.

tion factor; $p14^{ARF}$ has been shown to interact with and inhibit the transcriptional activity of the c-Myc oncogene (53, 54).

Our findings extend and help clarify recent reports that describe the ARF-B23 association and thus implicate ARF in the regulation of protein synthesis. Data demonstrating that the murine homologue of $p14^{ARF}$, $p19^{ARF}$, promoted the degradation of B23 (31) and inhibited rRNA processing is not supported by our findings with $p14^{ARF}$ or indeed with other studies (21, 55). We found that B23 and ARF associate within the nucleolar pre-60 S ribosome, and it has been reported that nucleolar B23 is resistant to ARF-induced degradation (31). It has also been suggested that the interaction of $p19^{ARF}$ and B23 retains both proteins in the nucleolus, effectively impeding the nucleocytoplasmic shuttling of B23 to induce growth arrest (55) but also blocking $p19^{ARF}$-mediated p53 activation (21). Importantly, hdm2 and B23 compete for ARF binding, and thus silencing of B23 expression enhanced the ARF-mdm2 association within the nucleoplasm and induced p53-activated growth arrest (19). The implications of these findings are that $p19^{ARF}$ directly accesses ribosome function through its nucleolar association with B23 and that it regulates the p53 cell cycle pathway via its nucleoplasmic interaction with hdm2.

This model is supported by our studies with human $p14^{ARF}$. We have shown that the predominantly nucleolar $p14^{ARF}$ was associated with B23 within the 60 S preribosome subunit, and this interaction did not involve hdm2 or p53, both of which were excluded from nucleoli and the preribosomes. Further, the ARF-mediated inhibition of protein translation *in vivo* supports the notion that ARF modulates ribosome function. We propose that ARF is a highly mobile protein, and as it accumulates in response to oncogenic activity, the increased nucleoplasmic fraction complexes hdm2, in preference to B23 (55), and activates p53-mediated growth arrest. Likewise, a fraction of nucleolar ARF, possibly a fraction tethered to B23, may impact ribosomes within the nucleolus. This work extends the already diverse functional repertoire of ARF to that of effects on protein translation; thus, ARF may serve to coordinate the regulation of cellular growth with that of proliferation. When these programs become uncoupled, as reported in T-ALL cells reconstituted to express $p16^{INK4a}$ (56), cells undergo proliferative arrest but continue to grow and differentiate.

There is strong precedent for the involvement of nucleolar proteins in the regulation of cell proliferation and cell growth. Nucleolar release of the ribosomal proteins L23, L11, and L5 promotes their interaction with hdm2, resulting in hdm2 inactivation and stabilization of p53. Similarly, the nucleolar protein Bop1 inhibits rRNA formation and also activates p53-dependent cell cycle arrest (38, 57). Analogous to ARF, nucleolar B23 contributes to multiple steps in ribosome biogenesis (58), and its nucleoplasmic redistribution activates p53 by inhibiting hdm2 (27). In all cases, these nucleolar regulators can rapidly halt cell cycle progression by leaching out of the nucleolus and signaling through the p53 pathway and also regulate the activity of ribosomes. We found that $p14^{ARF}$ promoted p53 activity and cell cycle arrest within 16 h of induction (the percentage of S phase inhibition in U20S_ARF cells induced for 16 h was 47%), whereas the ability of ARF to limit translation was not observed until 3 days after it was induced. This is consistent with the slower growth inhibitory impact of $p14^{ARF}$ expression in p53-null cells (59). Although $p14^{ARF}$ can alter ribosome function in the absence of p53, it is likely that inhibition of translation is enhanced in the presence of both $p14^{ARF}$ and p53, because both tumor suppressors independently inhibit ribosome function (60). The impact of p53 on translation is minor, however, and requires the inter-

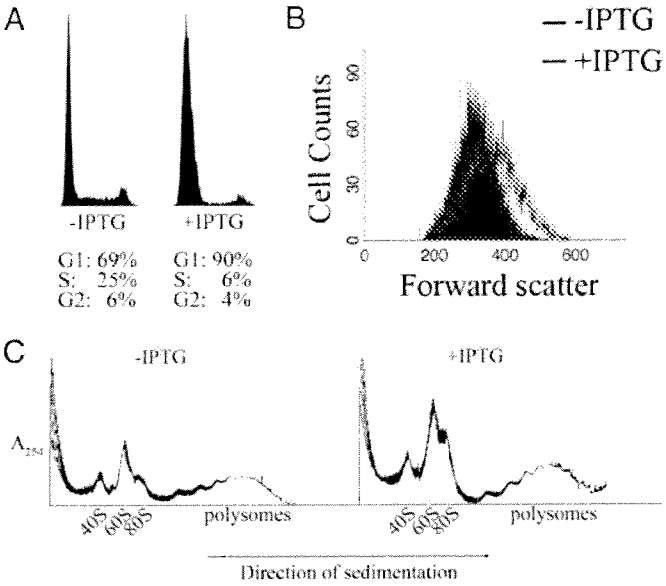

FIGURE 7. **p16^{INK4a} expression induces cell cycle arrest, increased cell size, and polysome formation.** *A*, cell cycle distribution of WMM1175_p16^{INK4a} cells either untreated or treated for 72 h with 5 mM IPTG using propidium iodide staining. *B*, flow cytometric forward scatter profiles of uninduced and induced cells. *C*, cytoplasmic ribosomes were fractionated on 10–45% sucrose density gradients with continuous monitoring of absorbance at 254 nm.

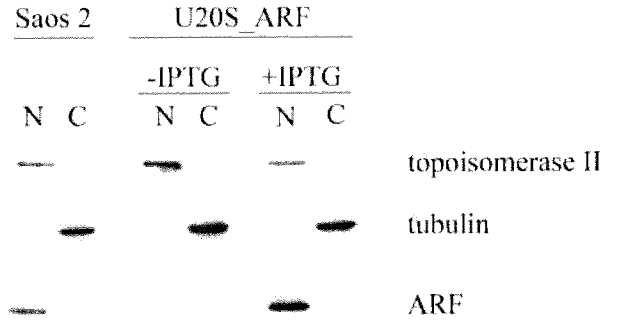

FIGURE 8. **p14^{ARF} protein accumulates in the nuclear fraction.** Saos 2 cells, uninduced U20S_ARF and IPTG-induced U20S_ARF cells were partitioned into Nonidet P-40 soluble cytosol (*C lanes*) and soluble nuclear (*N lanes*) fractions. Proteins corresponding to equal cell numbers were fractionated using SDS-PAGE and immunoblotted for the indicated proteins. The effective fractionation of cells was verified using antibodies against nuclear topoisomerase II and cytoplasmic tubulin.

action of p53 with polyribosomes (61), an association that we did not observe in ARF-expressing U20S cells (data not shown).

The increasing number of nucleolar proteins involved in regulating both ribosome biogenesis and p53 function emphasizes the pivotal role of the nucleolus in synchronizing cell cycle progression and cell growth. The majority of stress signals disrupt the nucleolus, causing the release of many proteins, including p14^{ARF}, B23, L11, L23, and L5, which interact with and inhibit hdm2 and thus activate p53. Despite the many functional similarities within this group of proteins, there is strong evidence of functional diversity. For instance, B23 appears necessary for UV-induced activation of p53 (27), L23 is important for actinomycin D-caused p53 induction (25), and p14^{ARF}, although not required for UV- or actinomycin-induced p53, is essential for the activation of p53 in response to oncogenes. In fact, the role of p14^{ARF} in response to hyperproliferative oncogenic signals may account for its ribosome regulatory function. Expression of p14^{ARF} is induced by the same oncogenes (Myc and Ras) that rapidly increase rRNA transcription rates (62, 63). Thus, in cells expressing activated oncogenes, the increased expression of p14^{ARF} would dampen the aberrant up-regulation of ribosome subunits. In contrast, in the absence of p14^{ARF}, oncogenic stimulation would promote increased ribosome biogenesis, enhanced translation rates, and ultimately transformation.

Acknowledgments—We thank Eileen McGowan and Stuart Gallagher for generating the U20S_ARF and WMM1175_ARF cell clones. We are also grateful to Neil Perkins for generously providing cell lines and Dimitri Pestov for helpful discussion.

REFERENCES

1. Kefford, R., Bishop, J. N., Tucker, M., Bressac-de Paillerets, B., Bianchi-Scarra, G., Bergman, W., Goldstein, A., Puig, S., Mackie, R., Elder, D., Hansson, J., Hayward, N., Hogg, D., and Olsson, H. (2002) *Lancet Oncol.* **3,** 653–654
2. Duro, D., Bernard, O., Della Valle, V., Berger, R., and Larsen, C. J. (1995) *Oncogene* **11,** 21–29
3. Stone, S., Jiang, P., Dayananth, P., Tavtigian, S. V., Katcher, H., Parry, D., Peters, G., and Kamb, A. (1995) *Cancer Res.* **55,** 2988–2994
4. Quelle, D. E., Zindy, F., Ashmun, R. A., and Sherr, C. J. (1995) *Cell* **83,** 993–1000
5. Krimpenfort, P., Quon, K. C., Mooi, W. J., Loonstra, A., and Berns, A. (2001) *Nature* **413,** 83–86
6. Sharpless, N. E., Bardeesy, N., Lee, K.-H., Carrasco, D., Castrillon, D. H., Aguirre, A. J., Wu, E. A., Horner, J. W., and DePinho, R. A. (2001) *Nature* **413,** 86–91
7. Kamijo, T., Zindy, F., Roussel, M. F., Quelle, D. E., Downing, J. R., Ashmun, R. A., Grosveld, G., and Sherr, C. J. (1997) *Cell* **91,** 649–659
8. Chin, L., Pomerantz, J., Polsky, D., Jacobson, M., Cohen, C., Cordon-Cardo, C., Horner, J. W. N., and DePinho, R. A. (1997) *Genes Dev.* **11,** 2822–2834
9. Freedberg, D. E., Mistry, S., Russak, J., Gai, W., Kaplow, M., Osman, I., Turner, F., Houghton, A., Busam, K. J., Bishop, T., Bastian, B. C., Newton Bishop, J. A., and Polsky, D. (2004) *Second Melanoma Research Congress,* Phoenix, AZ
10. Randerson-Moor, J. A., Harland, M., Williams, S., Cuthbert-Heavens, D., Sheridan, E., Aveyard, J., Sibley, K., Whitaker, L., Knowles, M., Newton Bishop, J., and Bishop, D. T. (2001) *Human Mol. Genet.* **10,** 55–62
11. Rizos, H., Darmanian, A. P., Holland, E. A., Mann, G. J., and Kefford, R. F. (2001) *J. Biol. Chem.* **276,** 41424–41434
12. Harland, M., Taylor, C. F., Chambers, P. A., Kukalizch, K., Randerson-Moor, J. A., Gruis, N. A., de Snoo, F. A., ter Huurne, J. A., Goldstein, A. M., Tucker, M. A., Bishop, D. T., and Bishop, J. A. (2005) *Oncogene.* **24,** 4604–4608
13. Laud, K., Marian, C., Avril, M. F., Barrois, M., Chompret, A., Goldstein, A. M., Tucker, M. A., Clark, P. A., Peters, G., Chaudru, V., Demenais, F., Spatz, A., Smith, M. W., Lenoir, G. M., and Bressac-de Paillerets, B. (2005) *J. Med. Genet.* **43,** 39–47
14. Stott, F. J., Bates, S., James, M. C., McConnell, B. B., Starborg, M., Brookes, S., Palmero, I., Ryan, K., Hara, E., Vousden, K. H., and Peters, G. (1998) *EMBO J.* **17,** 5001–5014
15. Kamijo, T., Weber, J. D., Zambetti, G., Zindy, F., Roussel, M. F., and Sherr, C. J. (1998) *Proc. Natl. Acad. Sci. U. S. A.* **95,** 8292–8297
16. Zhang, Y., Xiong, Y., and Yarbrough, W. G. (1998) *Cell* **92,** 725–734
17. Pomerantz, J., Schreiber-Agus, N., Liégeois, N. J., Silverman, A., Alland, L., Chin, L., Potes, J., Chen, K., Orlow, I., Lee, H.-W., Cordon-Cardo, C., and DePinho, R. A. (1998) *Cell* **92,** 713–723
18. Weber, J. D., Taylor, L. J., Roussel, M. F., Sherr, C. J., and Bar-Sagi, D. (1999) *Nat. Cell Biol.* **1,** 20–26

19. Korgaonkar, C., Zhao, L., Modestou, M., and Quelle, D. E. (2002) *Mol. Cell Biol.* **22,** 196–206
20. Llanos, S., Clark, P. A., Rowe, J., and Peters, G. (2001) *Nat. Cell Biol.* **3,** 445–452
21. Korgaonkar, C., Hagen, J., Tompkins, V., Frazier, A. A., Allamargot, C., Quelle, F. W., and Quelle, D. E. (2005) *Mol. Cell Biol.* **25,** 1258–1271
22. Rubbi, C. P., and Milner, J. (2003) *EMBO J.* **22,** 6068–6077
23. Zhang, Y., Wolf, G. W., Bhat, K., Jin, A., Allio, T., Burkhart, W. A., and Xiong, Y. (2003) *Mol. Cell Biol.* **23,** 8902–8912
24. Jin, A., Itahana, K., O'Keefe, K., and Zhang, Y. (2004) *Mol. Cell Biol.* **24,** 7669–7680
25. Dai, M. S., Zeng, S. X., Jin, Y., Sun, X. X., David, L., and Lu, H. (2004) *Mol. Cell Biol.* **24,** 7654–7668
26. Dai, M. S., and Lu, H. (2004) *J. Biol. Chem.* **279,** 44475–44482
27. Kurki, S., Peltonen, K., Latonen, L., Kiviharju, T. M., Ojala, P. M., Meek, D., and Laiho, M. (2004) *Cancer Cell* **5,** 465–475
28. Rodway, H., Llanos, S., Rowe, J., and Peters, G. (2004) *Oncogene* **23,** 6186–6192
29. Sugimoto, M., Kuo, M.-L., Roussel, M. F., and Sherr, C. J. (2003) *Mol. Cell* **11,** 415–424
30. Bertwistle, D., Sugimoto, M., and Sherr, C. J. (2004) *Mol. Cell Biol.* **24,** 985–996
31. Itahana, K., Bhat, K. P., Jin, A., Itahana, Y., Hawke, D., Kobayashi, R., and Zhang, Y. (2003) *Mol. Cell* **12,** 1151–1161
32. Savkur, R. S., and Olson, M. O. (1998) *Nucleic Acids Res.* **26,** 4508–4515
33. Lee, C., Smith, B. A., Bandyopadhyay, K., and Gjerset, R. A. (2005) *Cancer Res.* **65,** 9834–9842
34. Rizos, H., Darmanian, A. P., Indsto, J. O., Shannon, J. A., Kefford, R. F., and Mann, G. J. (1999) *Melanoma Res.* **9,** 10–19
35. Gallagher, S., Kefford, R. F., and Rizos, H. (2004) *Cell Cycle* **4,** 465–472
36. Becker, T. M., Rizos, H., Kefford, R. F., and Mann, G. J. (2001) *Clin. Cancer Res.* **7,** 3282–3288
37. Lutsch, G., Stahl, J., Kargel, H. J., Noll, F., and Bielka, H. (1990) *Eur. J. Cell Biol.* **51,** 140–150
38. Strezoska, Z., Pestov, D. G., and Lau, L. F. (2000) *Mol. Cell Biol.* **20,** 5516–5528
39. Diller, L., Kassel, J., Nelson, C. E., Gryka, M. A., Litwak, G., Gebhardt, M., Bressac, B., Ozturk, M., Baker, S. J., Vogelstein, B., and Friend, S. H. (1990) *Mol. Cell Biol.* **10,** 5772–5781
40. Martelli, F., Hamilton, T., Silver, D. P., Sharpless, N. E., Bardeesy, N., Rokas, M., DePinho, R. A., Livingston, D. M., and Grossman, S. R. (2001) *Proc. Natl. Acad. Sci. U. S. A.* **98,** 4455–4460
41. Graff, J. R., and Zimmer, S. G. (2003) *Clin. Exp. Metastasis* **20,** 265–273
42. Ptushkina, M., von der Haar, T., Vasilescu, S., Frank, R., Birkenhager, R., and McCarthy, J. E. (1998) *EMBO J.* **17,** 4798–4808
43. Proud, C. G. (2005) *Semin. Cell Dev. Biol.* **16,** 3–12
44. Mao, X., Green, J. M., Safer, B., Lindsten, T., Frederickson, R. M., Miyamoto, S., Sonenberg, N., and Thompson, C. B. (1992) *J. Biol. Chem.* **267,** 20444–20450
45. Marissen, W. E., Guo, Y., Thomas, A. A., Matts, R. L., and Lloyd, R. E. (2000) *J. Biol. Chem.* **275,** 9314–9323
46. De Benedetti, A., Williams, G. J., Comeau, L., and Baglioni, C. (1985) *J. Virol.* **55,** 588–593
47. Bates, S., Phillips, A. C., Clark, P. A., Stott, F., Peters, G., Ludwig, R. L., and Vousden, K. H. (1998) *Nature* **395,** 124–125
48. Palmero, I., Pantoja, C., and Serrano, M. (1998) *Nature* **395,** 125–126
49. Zindy, F., Eischen, C. M., Randle, D. H., Kamijo, T., Cleveland, J. L., Sherr, C. J., and Roussel, M. F. (1998) *Genes Dev.* **12,** 2424–2433
50. Huang, N., Negi, S., Szebeni, A., and Olson, M. O. (2005) *J. Biol. Chem.* **280,** 5496–5502
51. Rosenwald, I. B. (1996) *Cancer Lett.* **102,** 113–123
52. Rosenwald, I. B. (2004) *Oncogene* **23,** 3230–3247
53. Datta, A., Nag, A., Pan, W., Hay, N., Gartel, A. L., Colamonici, O., Mori, Y., and Raychaudhuri, P. (2004) *J. Biol. Chem.* **279,** 36698–36707
54. Qi, Y., Gregory, M. A., Li, Z., Brousal, J. P., West, K., and Hann, S. R. (2004) *Nature* **431,** 712–717
55. Brady, S. N., Yu, Y., Maggi, L. B., and Weber, J. D. (2004) *Mol. Cell Biol.* **24,** 9327–9338
56. Ausserlechner, M. J., Obexer, P., Geley, S., and Kofler, R. (2005) *Leukemia* **19,** 1051–1057
57. Pestov, D. G., Strezoska, Z., and Lau, L. F. (2001) *Mol. Cell Biol.* **21,** 4246–4255
58. Ginisty, H., Amalric, F., and Bouvet, P. (1998) *EMBO J.* **17,** 1476–1486
59. Weber, J. D., Jeffers, J. R., Rehg, J. E., Randle, D. H., Lozano, G., Roussel, M. F., Sherr, C. J., and Zambetti, G. P. (2000) *Genes Dev.* **14,** 2358–2365
60. Horton, L. E., Bushell, M., Barth-Baus, D., Tilleray, V. J., Clemens, M. J., and Hensold, J. O. (2002) *Oncogene.* **21,** 5325–5334
61. Yin, X., Fontoura, B. M., Morimoto, T., and Carroll, R. B. (2003) *J. Cell Physiol.* **196,** 474–482
62. Arabi, A., Wu, S., Ridderstrale, K., Bierhoff, H., Shiue, C., Fatyol, K., Fahlen, S., Hydbring, P., Soderberg, O., Grummt, I., Larsson, L. G., and Wright, A. P. (2005) *Nat. Cell Biol.* **7,** 303–310
63. Stefanovsky, V. Y., Pelletier, G., Hannan, R., Gagnon-Kugler, T., Rothblum, L. I., and Moss, T. (2001) *Mol. Cell* **8,** 1063–1073